ISSN 1349-1113
JAXA-RR-04-024E

JAXA Research and Development Report

Non-contact thermophysical property measurements of refractory metals using an electrostatic levitator

Takehiko ISHIKAWA, Paul-François PARADIS,
Toshio ITAMI and Shinichi YODA

March 2005

Japan Aerospace Exploration Agency

Non-contact thermophysical property measurements of refractory metals using an electrostatic levitator

By

Takehiko Ishikawa[1], Paul-François Paradis[1], Toshio Itami[2], and Shinichi Yoda[1]

Abstract : The electrostatic levitation system, including its history and development, and techniques for non-contact thermophysical property measurements (density, surface tension, and viscosity) are reviewed. Thermophysical properties of refractory metals whose melting temperatures are over 2, 000 K have been measured with an electrostatic levitator. The experimental results for vanadium, zirconium, niobium, molybdenum, rhodium, ruthenium, iridium, tantalum, rhenium, tungsten, and rhenium are presented. Comparison between theoretical calculations based on hard sphere model and measured data, as well as the necessity of microgravity conditions for this research are also discussed.

Key words : containerless processing, undercool, density, surface tension, viscosity

1. Introduction

The use of a containerless technique for materials processing has many technological and scientific advantages. The absence of a crucible allows the handling of chemically reactive materials such as molten refractory metals, alloys, or semiconductors, and eliminates the risk of sample contamination in overheated as well as in undercooled states (liquid phase below melting temperature). This offers excellent opportunities to characterize the structure of materials and to determine accurately their thermophysical properties in those states. The lack of a crucible also suppresses nucleation induced by the walls of a container (heterogeneous nucleation) thus increasing the possibility of producing new materials such as metallic glasses.

Several levitation methods, including acoustic, electromagnetic, aerodynamic, and electrostatic have been applied for thermophysical property measurements. The electromagnetic levitation method has been most popularly used for metal samples because instrumentation is rather simple, and compatible with high vacuum. An electromagnetic levitation facility was developed for microgravity experiment onboard the space shuttle, and several thermophysical properties such as density, heat capacity, surface tension, viscosity, and electrical conductivity were successfully measured.[1-3)]

An alternative scheme for metal samples processing is electrostatic levitation. This method uses Coulomb force between a charged sample and electrodes and needs a high speed feedback control system in order to

[1]Japan Aerospace Exploration Agency (JAXA), 2-1-1 Sengen, Tsukuba, Ibaraki, 305-8505, Japan.

[2]Hokkaido University, faculty of Science, Department of Chemistry, Sapporo, 060 Japan.

stabilize sample position. Due to this technical difficulty, the development of electrostatic levitation method was slower than other methods.

Like other levitation methods, development of electrostatic levitation methods was mainly conducted by governmental space organizations.[4] In 1988, European Space Agency (ESA) performed the first microgravity experiment in sounding rocket (TEXUS-19), attempting to levitate and melt a glass forming material (24m% Li_2O-76m% SiO_2) with an electrostatic scheme.[5] This trial was unsuccessful, due to high speed sample position control difficulty. However, progress of computer technology made the high speed control possible.

Rhim et al. at the Jet Propulsion Laboratory (JPL) developed a ground base electrostatic levitation system[6] and successfully levitated and melted refractory metals (zirconium[7] and titanium[8]) and semiconductors (silicon[9] and germanium.[10]) His group also developed several techniques to measure thermophysical properties such as density[11], isobaric heat capacity[12], surface tension[13], viscosity[13], and electrical resistivity[14] with the electrostatic levitation system. This great work has diffused all over the world. Electrostatic levitators in Marshall Space Flight Center (MSFC/NASA) (built and donated by Space Systems/ Loral)[15, 16], in German Aerospace Center,[17] and in Japan Aerospace Exploration Agency (JAXA)[18] were all derived from his pioneering design and sample position sensing and control method.

We have been conducted our research for the electrostatic levitation furnace (ELF) in JAXA since 1992, as a part of experiment facility developments for the International Space Station (ISS). In 1998, we successfully levitated and melted a $BiFeO_3$ sample under pressurized conditions on-board a sounding rocket.[19] After the microgravity experiments, ground research has been focused on the following 2 items: (1) Levitation and thermophysical property measurements of oxide materials, and (2) thermophysical property measurements of refractory metals whose melting points are over 2, 000 K. Both of these items have not been fully accomplished by JPL.

2. Electrostatic levitation system

The ELF has been developed based on a design by Rhim et al.[6] with several modifications. **Fig. 1** depicts schematically this apparatus. It consisted of a stainless steel chamber that was evacuated to a pressure of around 10^{-5} Pa. The chamber housed a pair of parallel disk electrodes, typically 10 mm apart between which a positively charged sample was levitated. The top electrode was kept electrically negative. These electrodes were utilized to control the vertical position (z) of the specimen. The Coulomb force between the sample and these electrodes cancelled the gravity force. The typical sample size is 2mm in diameter and an electrical field of around 8 to 15 kV/m is necessary to levitate it against gravity. In addition, four spherical electrodes distributed around the bottom electrode were used for horizontal control (x and y). Also surrounding the lower electrode, were four coils that generated a rotating magnetic field, used to control sample rotation.[14]

Since the electrostatic scheme can not produce a potential minimum, feedback position control system was necessary. Position sensing was achieved with a set of orthogonally disposed He-Ne laser (632. 8 nm) that projected a sample image on position sensors. One sensor detected the y-z position whereas another one was dedicated to the x direction. **Fig. 2** illustrates the hardware arrangement for position control. The beam of a He-Ne laser was expanded and impinged on a levitated sample. The size of the resulting sample shadow was optimized with a lens to cover the area of the sensor such that a good dynamic range was obtained. In addition, a polarization filter was used to optimize the laser intensity reaching the sensor. The sensor was equipped with a band-pass filter at 632. 8 nm to eliminate the photon noise coming from sources other than the laser. The sample position

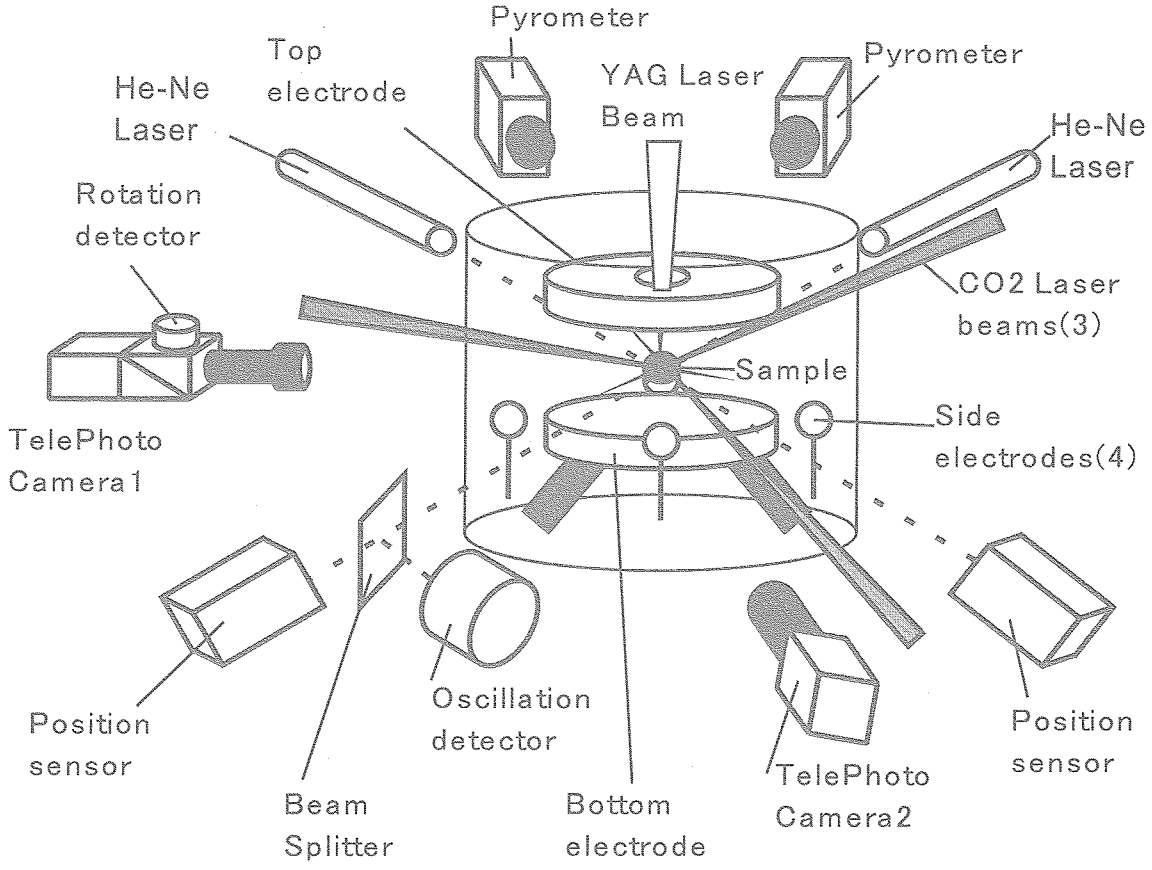

Fig.1 Schematic view of the electrostatic levitation furnace.

information read by the sensors was then fed to a computer and analyzed by a program. The program used PID servo algorithms for implementing the feedback system, thus allowing a sample to maintain a fixed position in time. The computer then imputed new values of voltages for each electrode. The feedback rate was 720 Hz for the z direction and 30 Hz for the x and y direction.

Sample heating was achieved using two 100 W CO_2 lasers emitting at 10. 6 μm and a 520 W Nd:YAG laser emitting at 1. 064 μm. The high power Nd:YAG laser was used to melt a sample with melting temperature higher than 2, 800 K (Mo, Ta, and Re). One CO_2 leaser beam was sent directly to the sample whereas the other CO_2 leaser beam was divided into two portions such that three focused beams, separated by 120 degrees in a horizontal plane, hit the sample. The Nd:YAG laser beam was sent to the sample from the vertical, through a hole in the top electrode. This quasi-tetrahedral multiple beam configuration minimized sample motion and enhanced temperature homogineity.[20)]

Sample temperature data were measured using single-color pyrometers (0. 90 μm and 0. 96μm, 120 Hz), equipped with a band stop filter (Rugate notch filter) at 1. 064 μm to remove any noise coming from the Nd:YAG laser. The levitated sample was observed by three charged-coupled-device cameras. One camera offered a view of both the electrodes and the sample. In addition, two black and white high-resolution cameras, located at right angle from each other and equipped with telephoto objectives in conjunction with background lamps, provided magnified views of the sample. This also helped to monitor the sample position in the horizontal plane and to align the heating laser beams to minimize any photon induced effects on the sample.

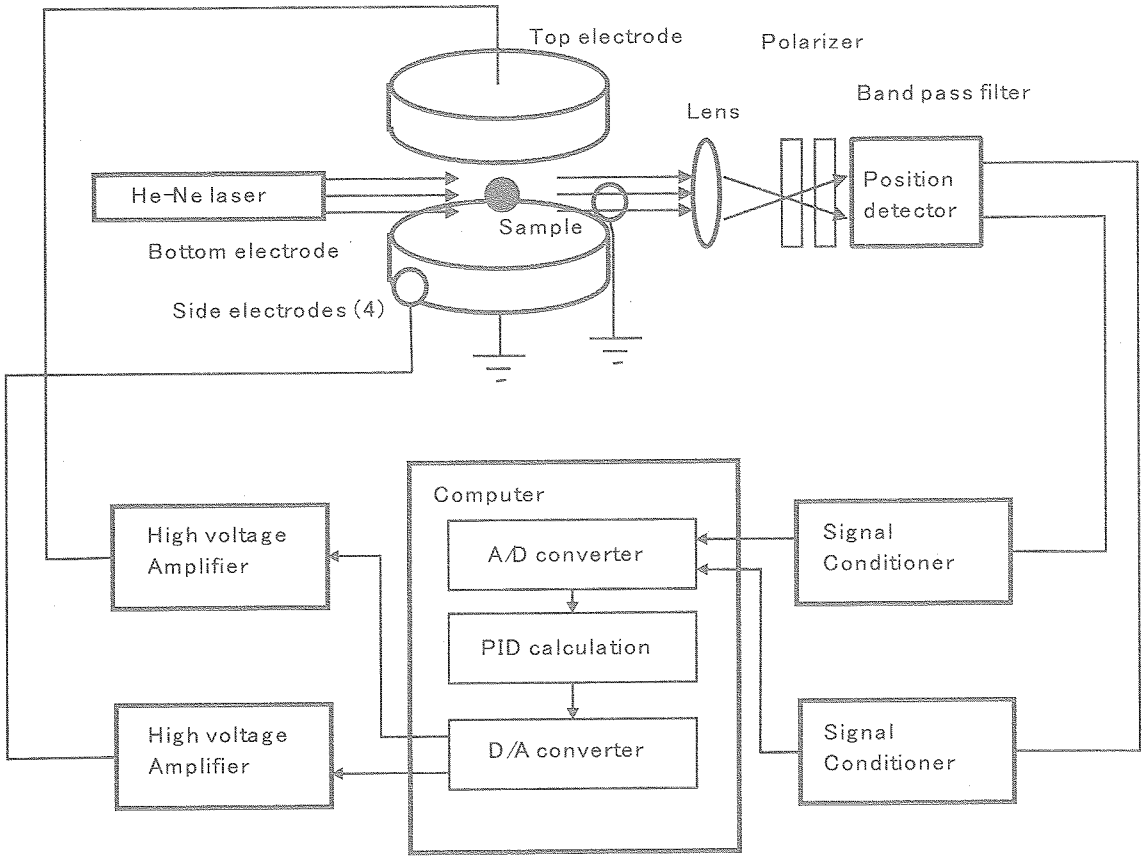

Fig.2 Schematic diagram on sample position control system of the electrostatic levitation.

A pressurized version of ELF[21] which can be operated up to 0. 45MPa was also developed by JAXA. The pressurized condition is necessary to suppress sample evaporation and maintain the stoichiometry of the sample, especially important for the oxide materials. We have successfully levitated and molten several oxide materials such as YAG and $BaTiO_3$. The results of the thermophysical property measurements of these materials can be found elsewhere.[22-24] This paper concentrates on the metal properties obtained with the high vacuum system.

3. Thermophysical properties measurements with the electrostatic levitation method

By combining such non-contact diagnostics apparatus as pyrometer or telephoto camera, several thermophysical properties can be measured with the electrostatic levitation furnace. Property measurements by containerless methods have several advantages compared with conventional methods. First, samples are free from the risk of contamination from the container, and materials with melting points higher than that of crucibles (e. g. platinum or alumina) can be processed. Second, since nucleation from the container wall can be suppressed, molten samples can be maintained in deeply undercooled condition.

3. 1. Density

The density and the ratio of isobaric heat capacity to hemispherical total emissivity were measured using a UV imaging technique[25] described in detail elsewhere and summarized below for completeness. Once the sample was molten, it took a spherical shape due to surface tension and the distribution of surface charge[26, 27]. If the shape of a liquefied sample departed from that of a sphere (due to excessive rotation), a counter torque was

applied by the rotating magnetic field. Since the sample was axi-symmetric and because the mass was known, density(ρ) could be calculated as;

$$\rho = \frac{3m}{4\pi r^3} \tag{1}$$

where m and r are mass and radius of the sample, respectively.

The radiance temperature measured by the pyrometer was calibrated by using recalescence of the sample (sudden temperature raise from undercooled temperature to the melting temperature (T_m) due to the release of latent heat of fusion). After the sample started to cool, both the images and the cooling curve were recorded to determine the density. The recorded video images were digitized and matched to the cooling curve. Then, a JAXA developed program extracted the area from each image and calculated the density at each temperature.

3. 2. Surface tension and viscosity

The surface tension and viscosity were determined by the drop oscillation method[13], for which the frequency of the surface oscillation of the levitated sample was measured around its equilibrium shape. In this method, a sample was molten and brought to a selected temperature. Then, a $P_2(cos\theta)$-mode of drop oscillation was induced to the sample by superimposing a small sinusoidal electric field on the levitation field. Here, $P_2(cos\theta)$ is a Legendre polynomial of 2nd order. An oscillation detection system, illustrated in **Fig. 3(a)**, measured the fluctuation of the vertical diameter of the molten sample[13] with 2000 Hz sampling frequency. The transient signal that followed the termination of the excitation field was shown in **Fig.3(b)**. This signal was analyzed using an in-house written LabVIEW™ program. This was done many times for a given temperature and repeated for several temperatures. Using the characteristic oscillation frequency ω_c of this signal after correcting for non-uniform surface charge distribution, the surface tension γ could be found from the following equation[13]

$$\omega_c^2 = \left(\frac{8\gamma}{\rho r_0^3}\right)\left(1 - \frac{Q^2}{64\pi^2 r_0^3 \gamma \varepsilon_0}\right)\{1 - f(\gamma, q, Y)\}, \tag{2}$$

where

$$f(\gamma, q, e) = \frac{(243.31\gamma^2 - 63.14q^2\gamma + 1.54q^4)Y^2}{176\gamma^3 - 120q^2\gamma^2 + 27\gamma q^4 - 2q^6}, \tag{3}$$

and r_0 is the radius of the sample when a spherical shape is assumed, ρ is the liquid density, Q is the drop charge, ε_0 is the permittivity of vacuum. The symbols q and Y are defined by

$$q^2 = \frac{Q^2}{16\pi^2 r_0^3 \varepsilon_0}, \tag{4}$$

and

$$Y^2 = E^2 r_0 \varepsilon_0, \tag{5}$$

respectively, and E is the applied electric field. The characteristic oscillation frequency ω_c of molten refractory metal droplet (*ca.* 2mm in diameter) ranged around 180 Hz to around 240 Hz.

Similarly, using the decay time τ given by the same signal, the viscosity η is found by[28]

$$\eta = \frac{\rho r_0^2}{5\tau}. \tag{6}$$

The liquid density data ρ is known by conducting measurements described in 3. 1, and radius of the sample r_0 can be determined by image analysis of the recorded sample image during oscillation experiment. The drop charge Q can be calculated by

$$mg = QE, \tag{7}$$

where g is the gravitational acceleration.

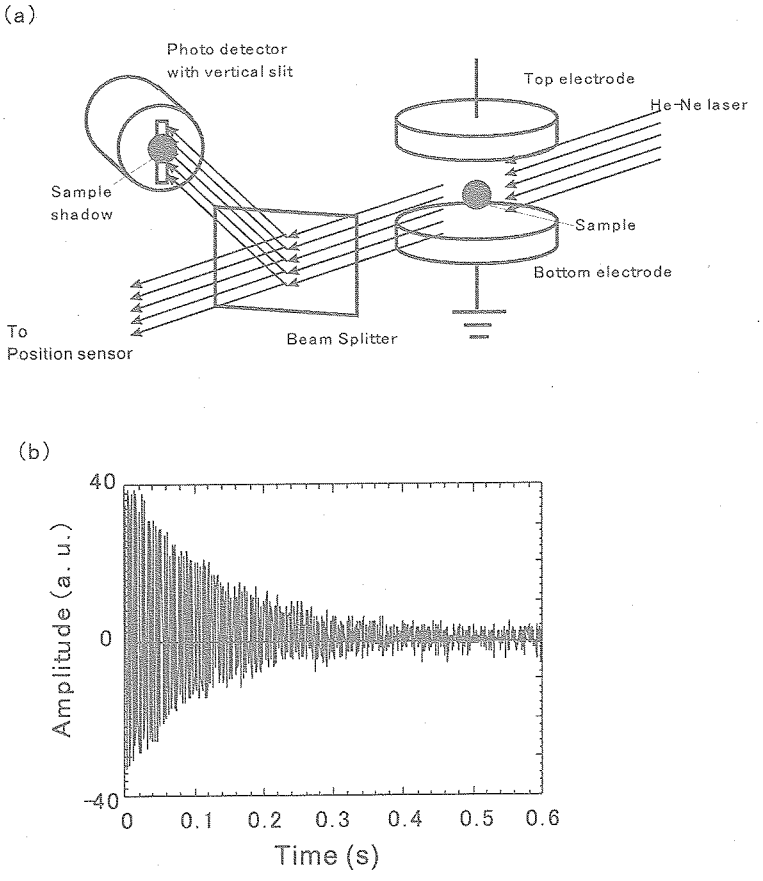

Fig.3 Sample oscillation detection for surface tension and viscosity measurement: (a) diameter sensing system and (b) signal of decay of the oscillation following electrical excitation for a molten sample measured by the diameter sensing system.

4. Result of thermophysical property measurement of refractory metals

4. 1. Density

The density data for each metal are listed in Table-1 to 11 and Fig.4 to 14 with literature values. During these experiments, the density was measured over large temperature range including regions above and below the melting temperature. The density, like that of other pure metals, exhibited a linear behavior as a function of temperature. In these measurements, the uncertainty was estimated to be less than 2% from the resolution of the video grabbing capability (640 x 480 pixels) and from the uncertainty in mass (±0.0001g).

Table 1 Literature values of the density for liquid vanadium

Metal T_m (K)	$\rho(T_m)$ (10^3kg·m^{-3})	$d\rho/dT$ (kg·m^{-3}K^{-1})	Temperature (K)	Reference
V	5.46	-0.49	1840-2240	Present work[29]
	5.55		2183	Allen[30]
2183	5.73		2208	Maurakh[31]
	5.36	-0.32	2200-2470	Saito[32]
	5.30		2183	Eljutin[33]
	5.57		2175-6600	Seydel[34]

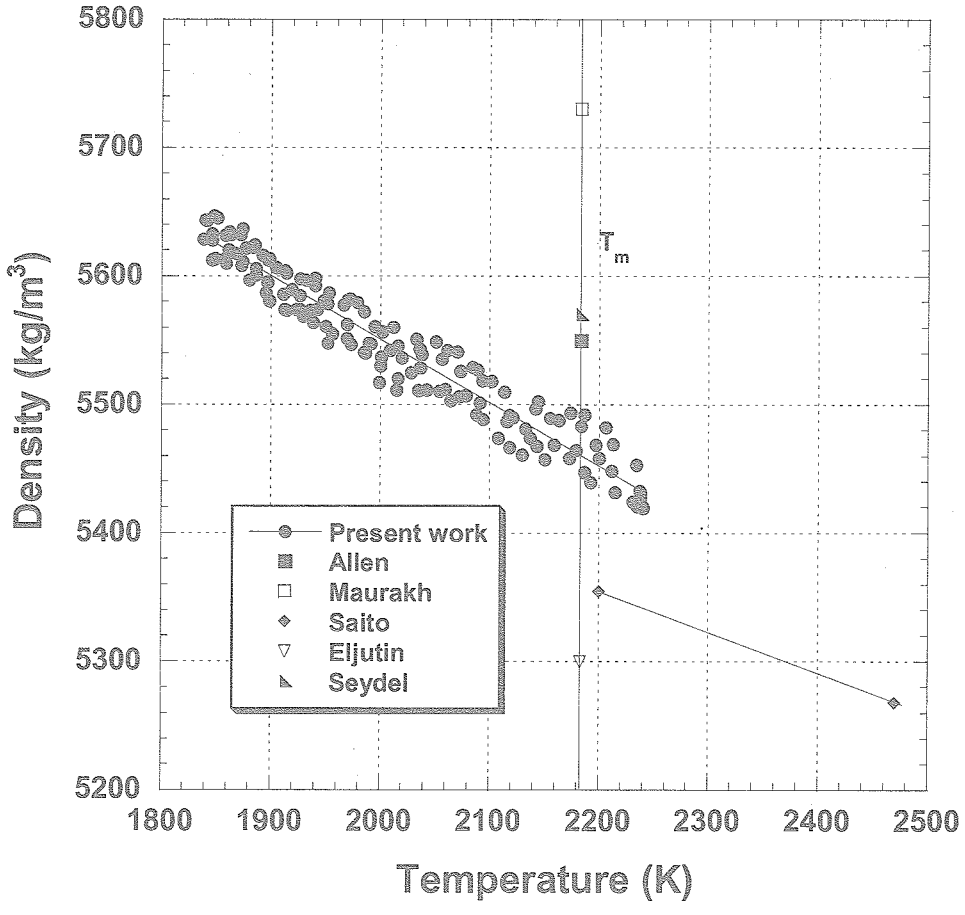

Fig.4 Density of liquid vanadium versus temperature.

Table 2 Literature values of the density for liquid zirconium

Metal T_m (K)	$\rho(T_m)$ (10^3kg·m^{-3})	$d\rho/dT$ (kg·m^{-3}K^{-1})	Temperature (K)	Reference
Zr	6.21	-0.27	1850-2750	Present work[35]
	5.80		2128	Allen[30]
2128	5.60		2128	Eljutin[33]
	6.06		2108	Maurakh[31]
	6.24	-0.29	1700-2300	Paradis[7]
	5.50		2125	Peterson[36]

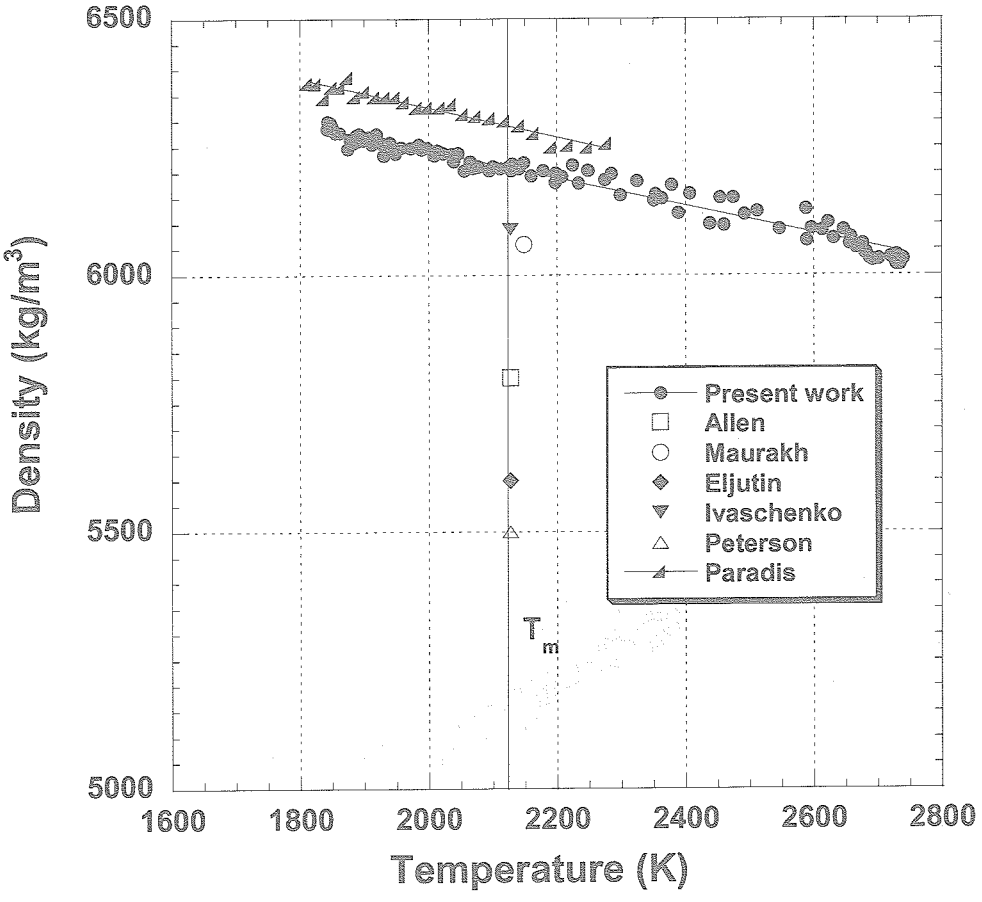

Fig.5 Density of liquid zirconium versus temperature.

Table 3 Literature values of the density for liquid niobium

Metal T_m (K)	ρ (T_m) (10^3kg·m^{-3})	$d\rho/dT$ (kg·m^{-3}K^{-1})	Temperature (K)	Reference
Nb	7.73	-0.39	2300-3000	Present work[35]
	7.83		2742	Allen[30]
2742	7.57		2742	Ivaschenko[37]
	7.6		2742	Eljutin[33]
	7.68	-0.54	2742	Shaner[38]

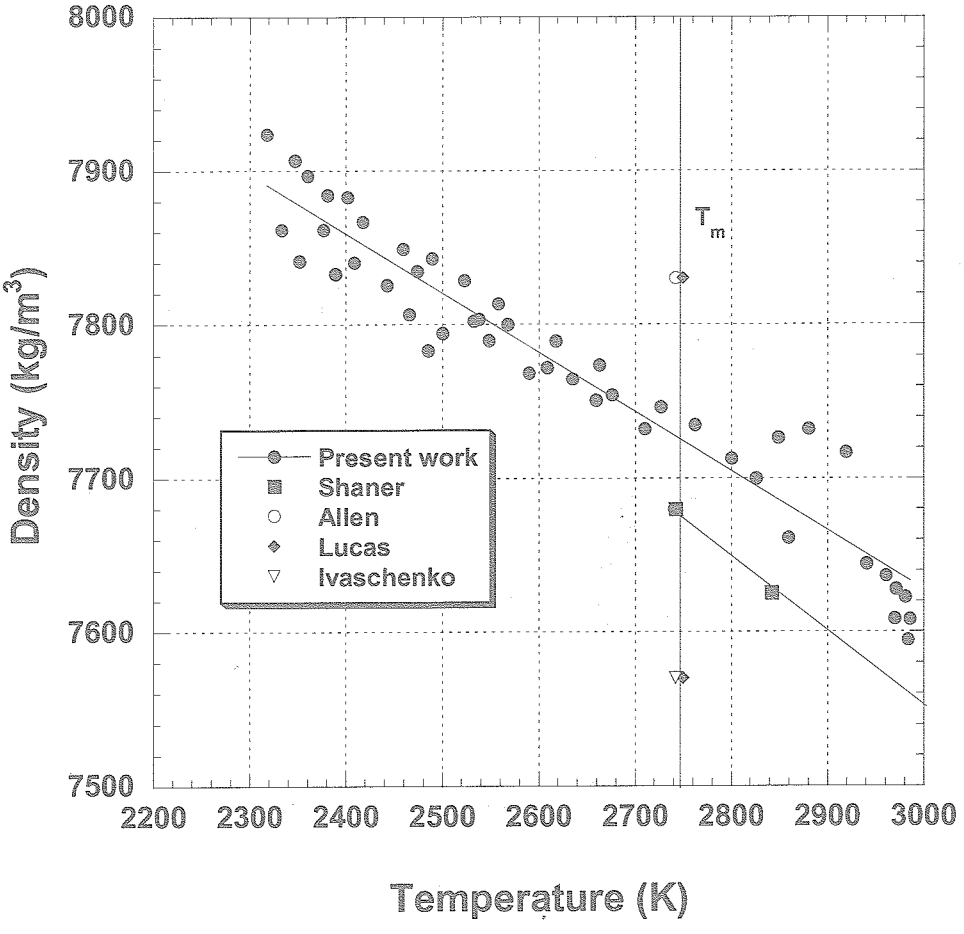

Fig.6 Density of liquid niobium versus temperature.

Table 4 Literature values of the density for liquid molybdenum

Metal T_m (K)	$\rho(T_m)$ (10^3kg·m^{-3})	$d\rho/dT$ (kg·m^{-3}K^{-1})	Temperature (K)	Reference
Mo	9.11	-0.60	2450-3000	Present work[39]
	9.35		2896	Allen[30]
2896	9.10		2896	Eljutin[33]
	9.33		2896	Pekarev[40]
	9.10	-0.80	2896-	Seydel[34]

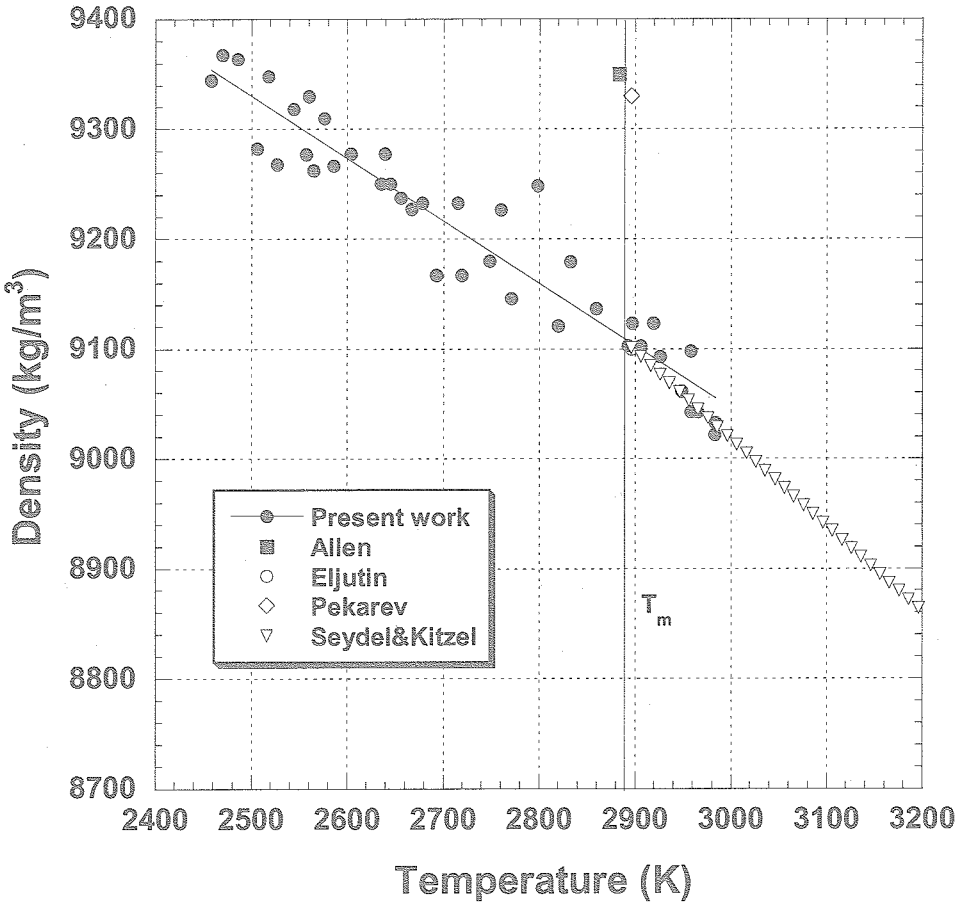

Fig.7 Density of liquid molybdenum versus temperature.

Table 5 Literature values of the density for liquid ruthenium

Metal T_m (K)	$\rho(T_m)$ (10^3kg·m^{-3})	$d\rho/dT$ (kg·m^{-3}K^{-1})	Temperature (K)	Reference
Ru 2607	10.75 10.9	-0.56	2225-2775 2607	Present work[41] Allen[30]

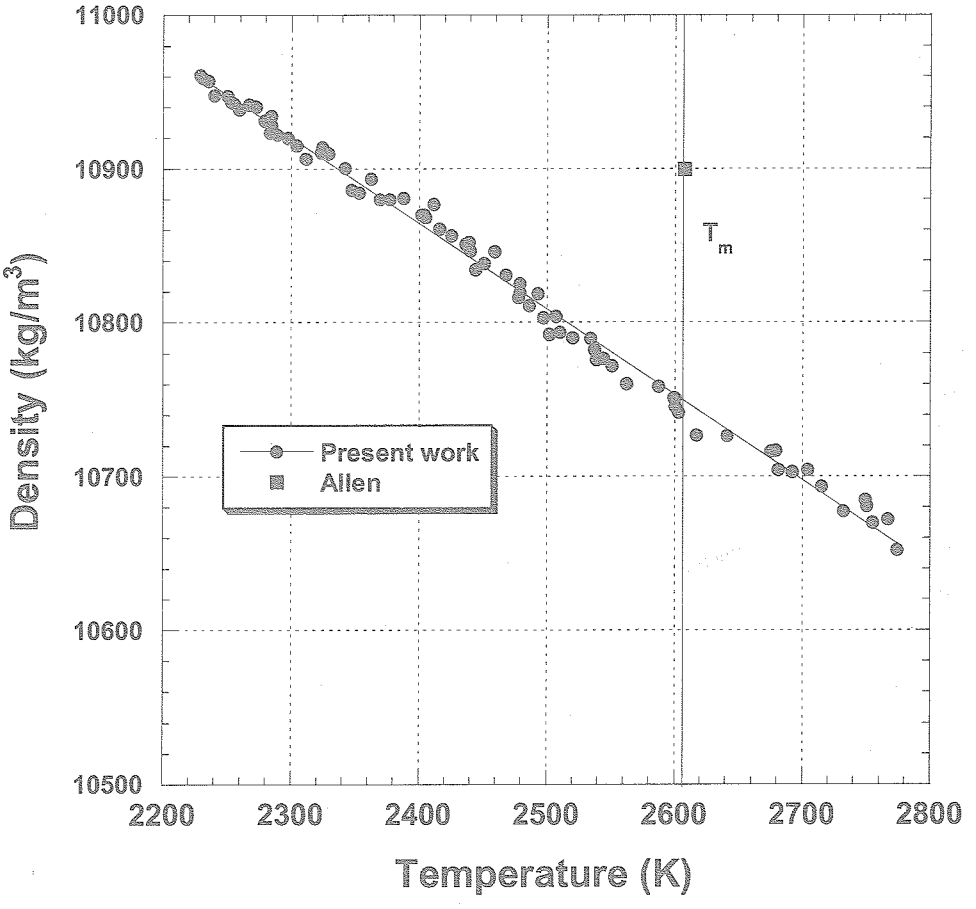

Fig.8 Density of liquid ruthenium versus temperature.

Table 6 Literature values of the density for liquid rhodium

Metal T_m (K)	$\rho(T_m)$ (10^3kg·m^{-3})	$d\rho/dT$ (kg·m^{-3}K^{-1})	Temperature (K)	Reference
Rh	10.82	-0.76	1820-2250	Present work[42]
	11.1		2236	Allen[30]
2236	10.65		2236	Eremenko[43]
	10.7	-0.90	2236-2473	Mitko[44]
	10.7		2236	Popel[45]
	12.2	-0.50	2236-2473	Dubinin[46]

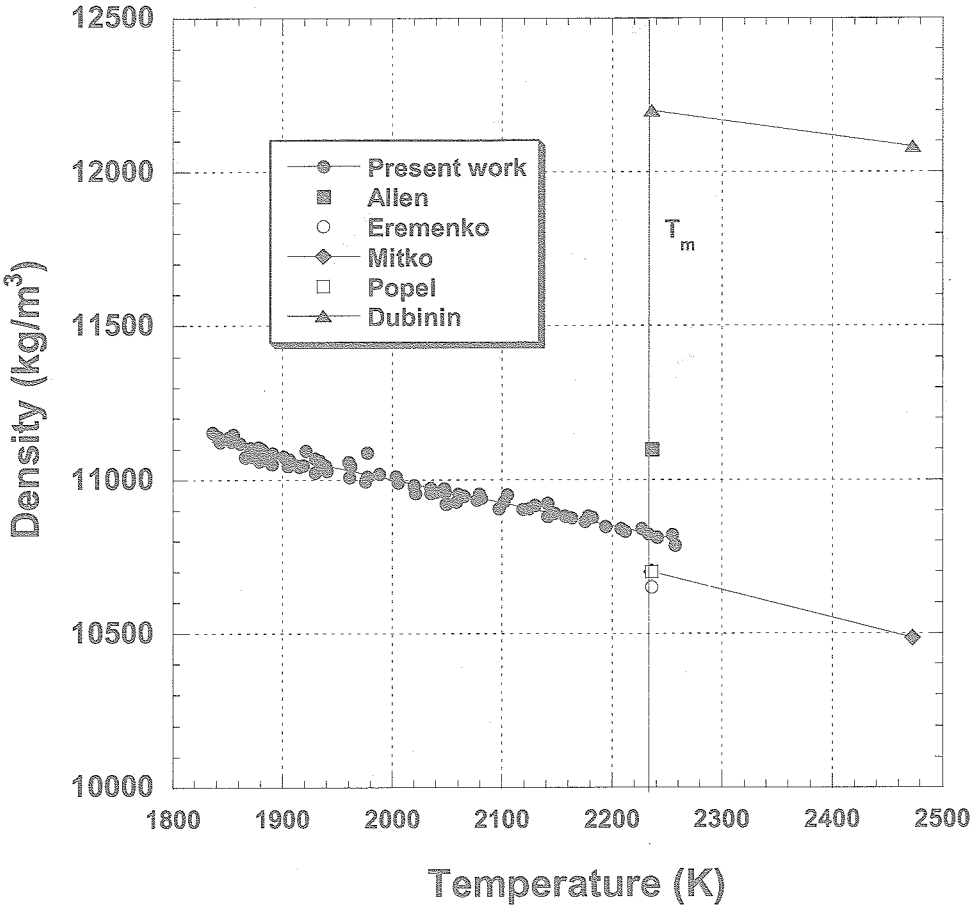

Fig.9 Density of liquid rhodium versus temperature.

Table 7 Literature values of the density for liquid hafnium

Metal T_m (K)	$\rho(T_m)$ (10^3kg·m^{-3})	$d\rho/dT$ (kg·m^{-3}K^{-1})	Temperature (K)	Reference
Hf	11.82	-0.55	2300-2700	Present work[47]
	12.0		2236	Allen[30]
2504	11.1		2504	Peterson[36]
	11.97		2504	Ivaschenko[48]
	11.5		2504	Arkhikin[49]

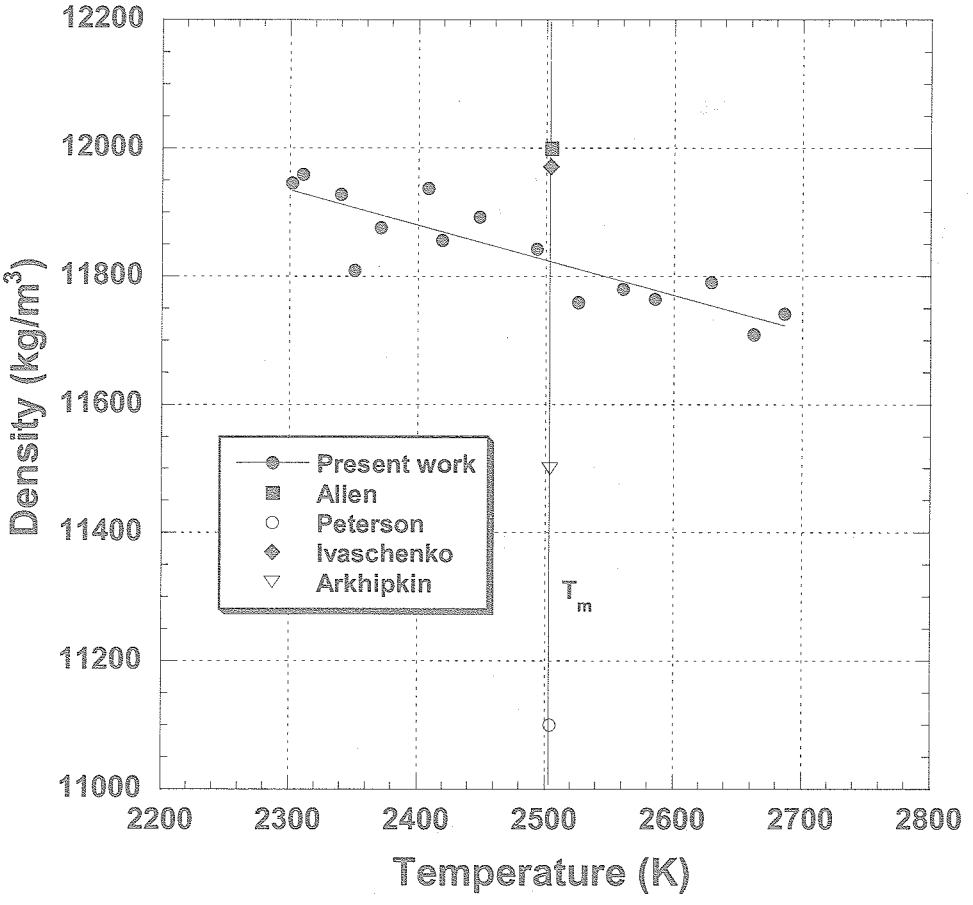

Fig.10 Density of liquid hafnium versus temperature.

Table 8 Literature values of the density for liquid tantalum

Metal T_m (K)	$\rho(T_m)$ (10^3kg·m^{-3})	$d\rho/dT$ (kg·m^{-3}K^{-1})	Temperature (K)	Reference
Ta	14.75	-0.85	2650-3420	Present work
	15.0		3290	Allen[30]
3290	14.43	-1.3		Shaner[38]
	14.6		3290	Berhault[51]

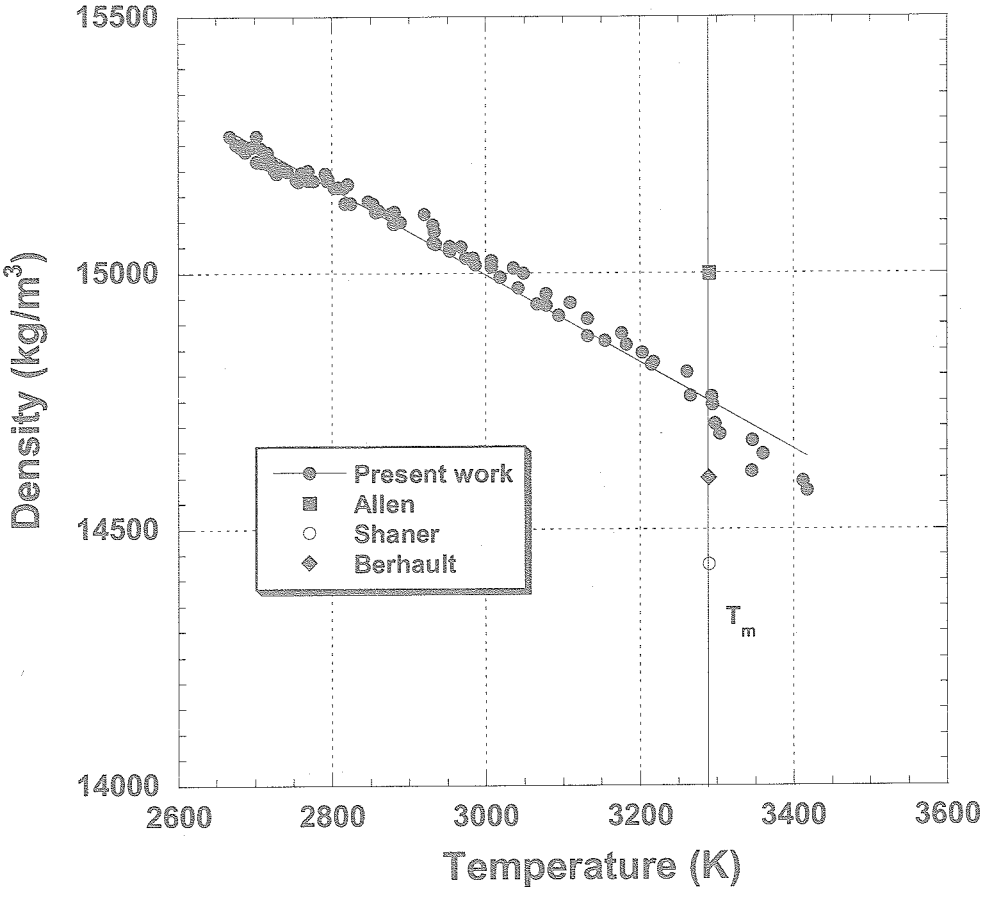

Fig.11 Density of liquid tantalum versus temperature.

Table 9 Literature values of the density for liquid tungsten

Metal T_m (K)	$\rho(T_m)$ (10^3kg·m^{-3})	$d\rho/dT$ (kg·m^{-3}K^{-1})	Temperature (K)	Reference
W	16.43	-1.08	3125-3707	Present work[52]
	17.5		3693	Allen[30]
3695	16.37	-0.97	3693-8000	Seydel[34]
	16.26		3693	Shaner[38]
	16.2		3693-5340	Berhault[51]
	17.6		3693	Calverley[53]

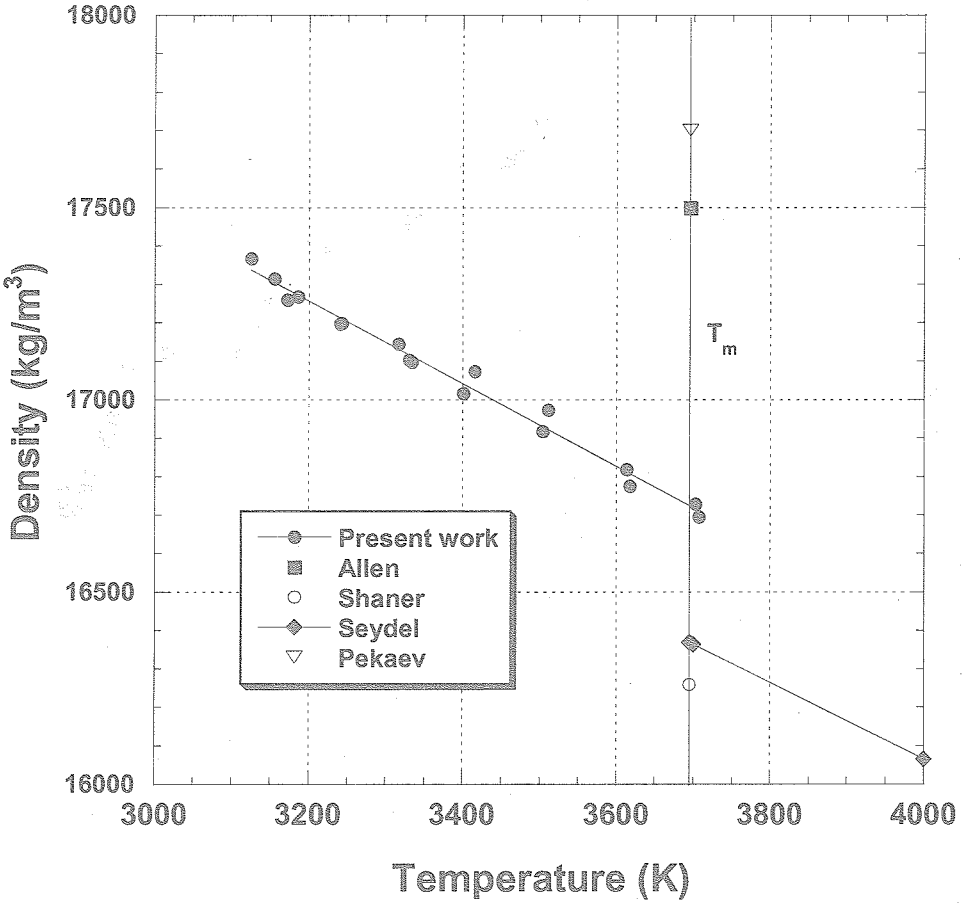

Fig.12 Density of liquid tungsten versus temperature.

Table 10 Literature values of the density for liquid rhenium

Metal T_m (K)	$\rho(T_m)$ (10^3kg·m^{-3})	$d\rho/dT$ (kg·m^{-3}K^{-1})	Temperature (K)	Reference
Re	18.65	-0.79	2683-3710	Present work[50]
	18.7		3459	Allen[30]
3459	18.0		3459	Thevenin[54]
	18.9		3459	Pekarev[40]

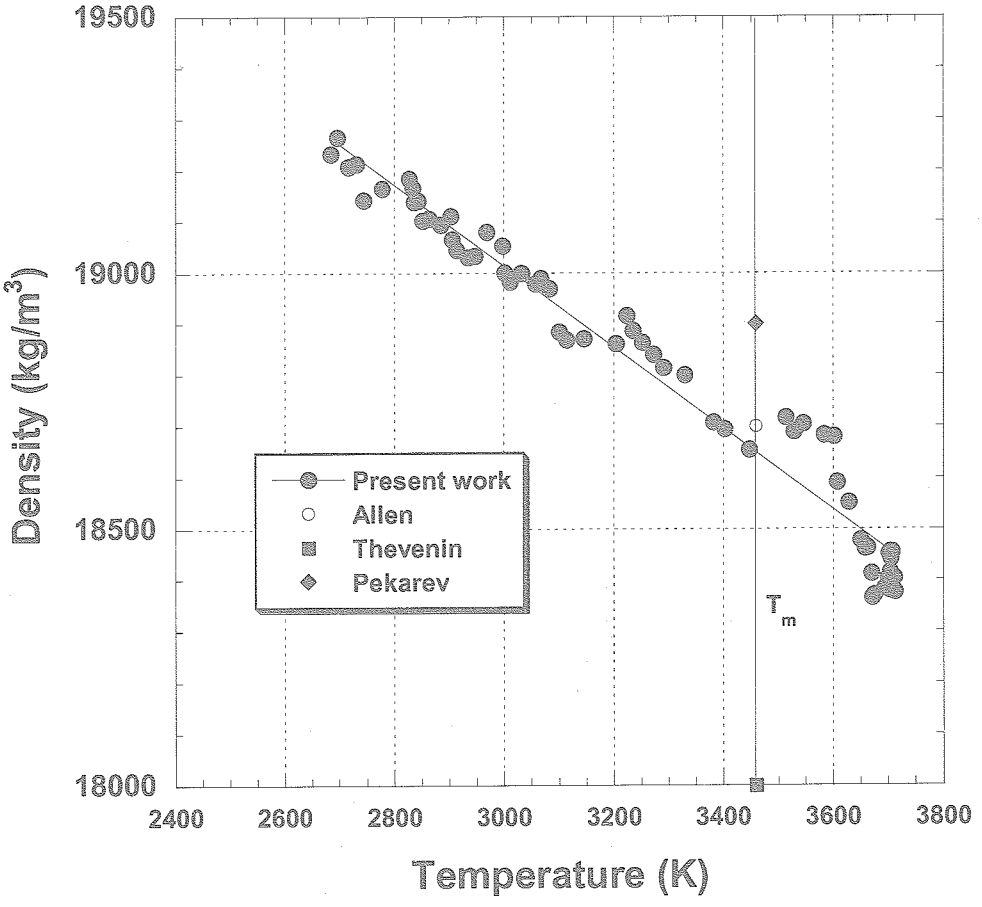

Fig.13 Density of liquid rhenium versus temperature.

Table 11 Literature values of the density for liquid iridium

Metal T_m (K)	$\rho(T_m)$ (10^3kg·m^{-3})	$d\rho/dT$ (kg·m^{-3}K^{-1})	Temperature (K)	Reference
Ir	19.87	-0.71	2300-3000	Present work[55]
	20.0		2719	Allen[30]
2719	19.39		2719	Martsenyuk[56]
	19.23		2723	Apollova [57]
	20.0		2719	Gathers[58]

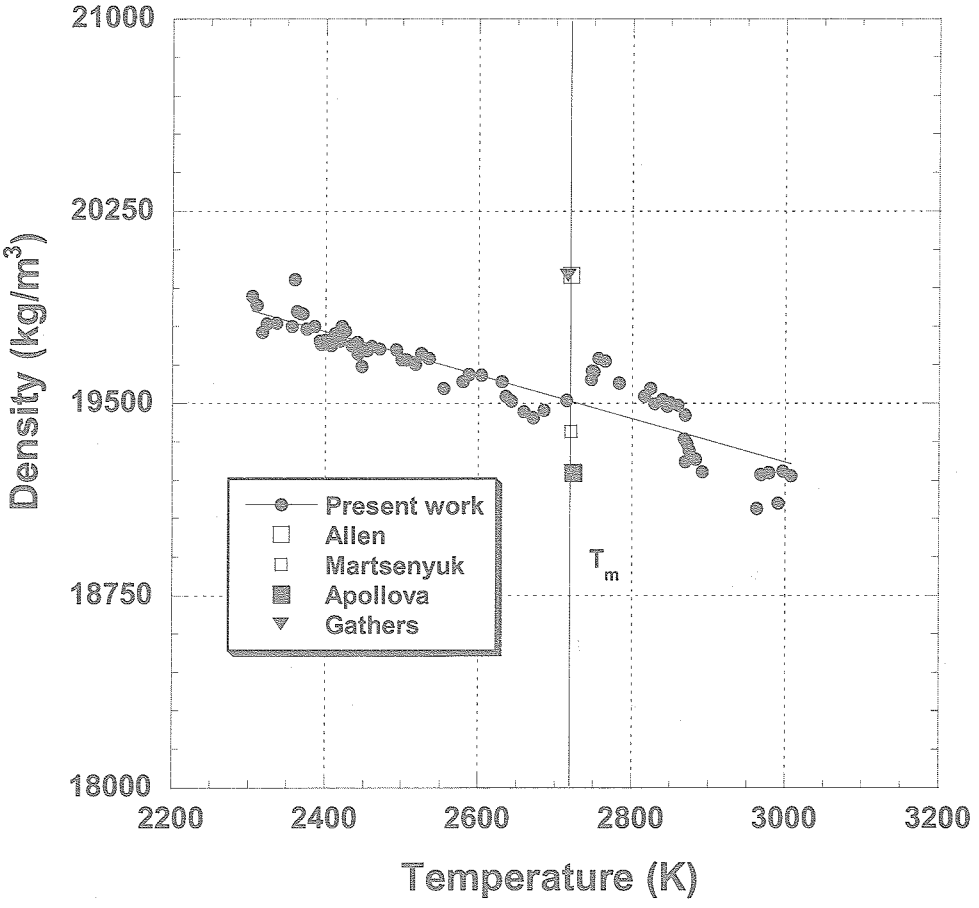

Fig.14 Density of liquid iridium versus temperature.

4. 2. Surface tension

The measured values and literature data for surface tension and viscosity are listed in Table-12 to 20 and Fig. 15 to 23. The surface tension could be measured over large temperature range including the undercooled phase in these experiments, whereas measurements by other methods could be done only around T_m. These tendencies become clearer for higher T_m samples.

Table 12 Literature values of the surface tension for zirconium

Metal T_m (K)	$\gamma(T_m)$ (10^{-3}N·m^{-1})	$d\gamma/dT$ (10^{-3}N·m^{-1}K^{-1})	Temperature (K)	Reference
Zr	1500	-0.11	1800-2400	Present work[59]
	1459	-0.24	1850-2200	Paradis[7]
2128	1512	-0.37		Egry[1]
	1480		2128	Allen[30]
	1400		2128	Peterson[36]
	1411		2128	Shunk[60]
	1430		2128	Kostikov[61]

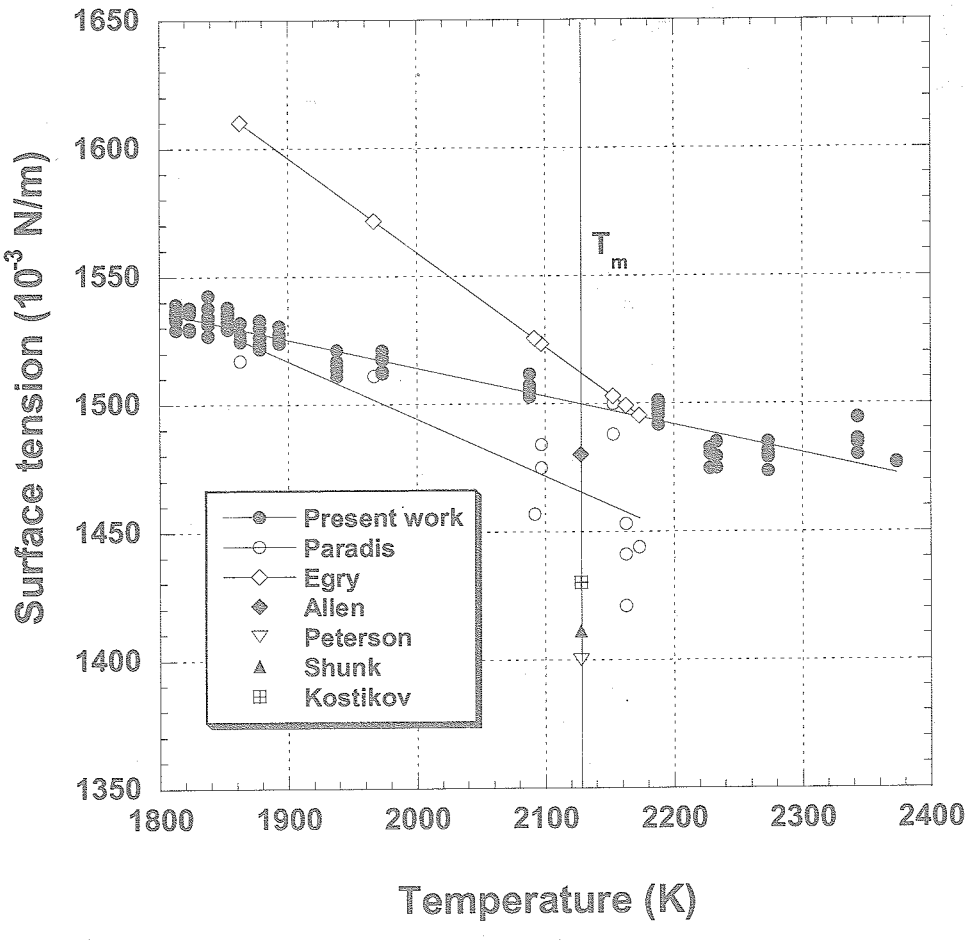

Fig.15 Surface tension of liquid zirconium versus temperature.

Table 13 Literature values of the surface tension for niobium

Metal T_m (K)	γ (T_m) (10^{-3}N·m^{-1})	dγ/dT (10^{-3}N·m^{-1}K^{-1})	Temperature (K)	Reference
Nb	1937	-0.20	2320-2915	Present work[59]
	1900		2742	Allen[30]
2742	1827		2742	Flint[62]
	1839		2742	Ivaschenko[63]
	2040		2742	Arkhipkin[64]
	1853		2472	Eremenko[65]

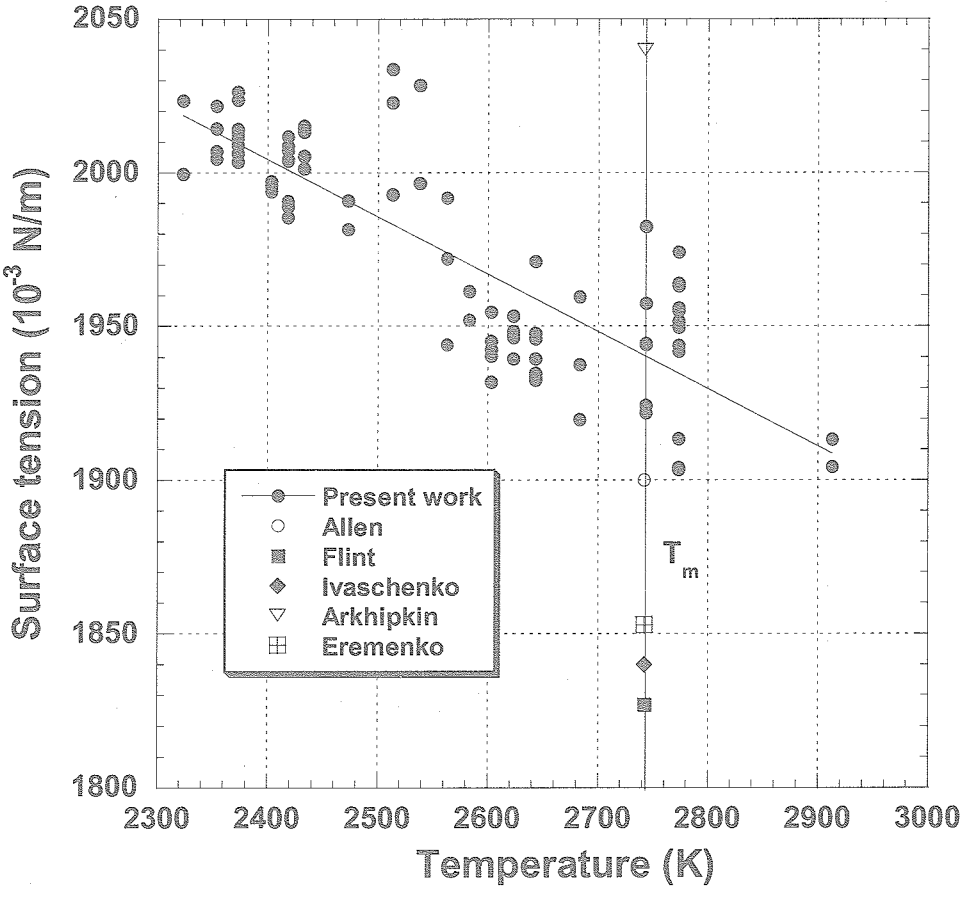

Fig.16 Surface tension of liquid niobium versus temperature.

Table 14 Literature values of the surface tension for ruthenium

Metal T_m (K)	$\gamma(T_m)$ (10^{-3}N·m^{-1})	$d\gamma/dT$ (10^{-3}N·m^{-1}K^{-1})	Temperature (K)	Reference
Ru 2607	2256	-0.24	2450-2725	Present work[41]
	2250		2607	Allen[30]
	2180		2607	Martensyuk[66]

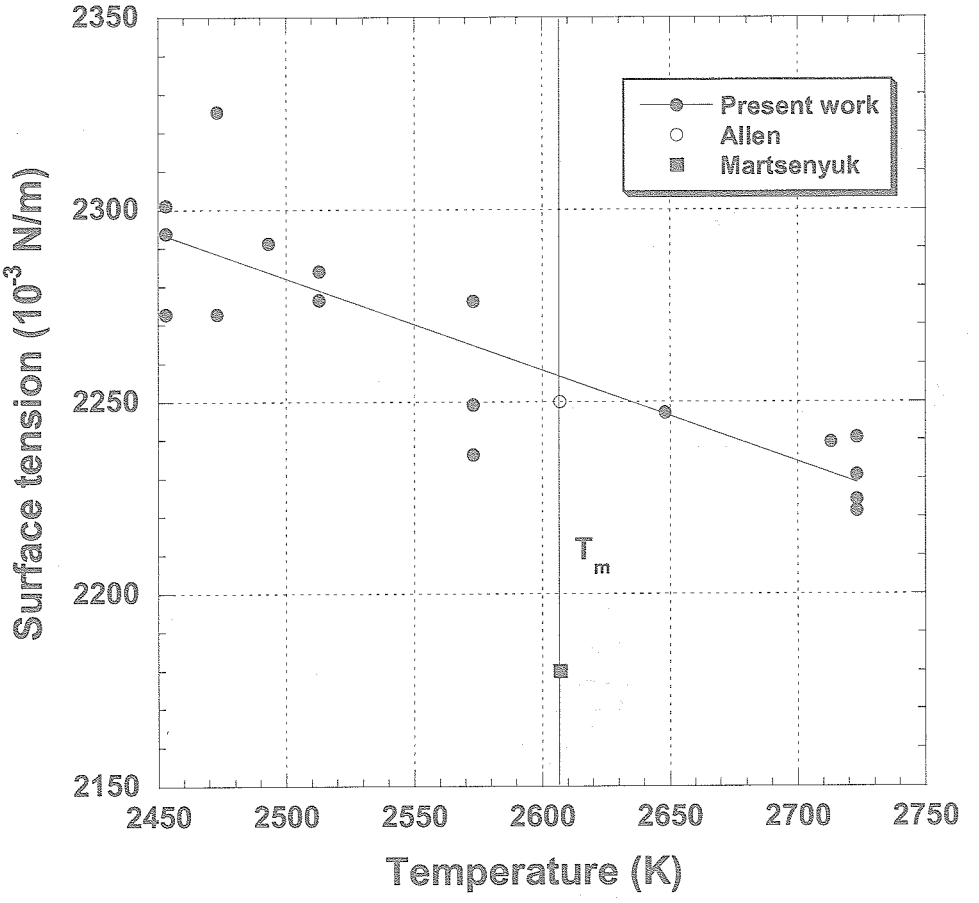

Fig.17 Surface tension of liquid ruthenium versus temperature.

Table 15 Literature values of the surface tension for rhodium

Metal T_m (K)	γ (T_m) (10^{-3}N·m^{-1})	dγ/dT (10^{-3}N·m^{-1}K^{-1})	Temperature (K)	Reference
Rh	1940	-0.30	1860-2380	Present work[42]
	2000		2236	Allen[30]
2236	1940		2236	Eremonko[43]
	1915	-0.664	2236-2473	Gushchin[67]

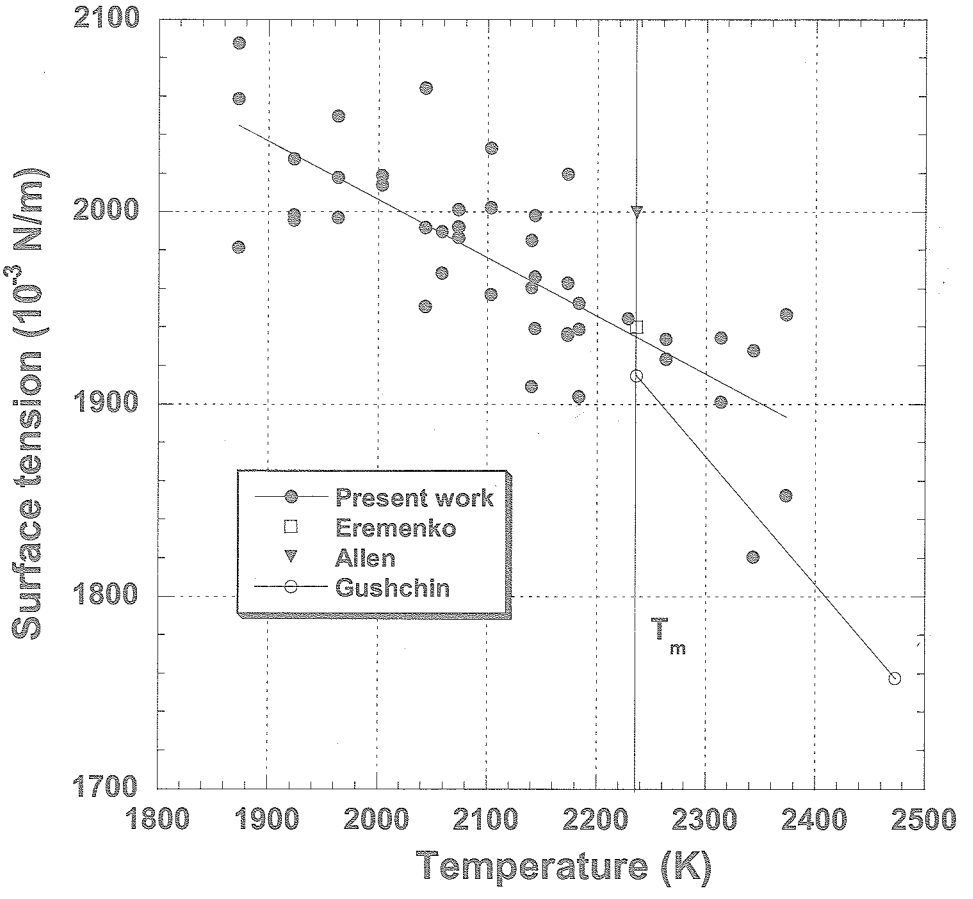

Fig.18 Surface tension of liquid rhodium versus temperature.

Table 16 Literature values of the surface tension for hafnium

Metal T_m (K)	γ (T_m) (10^{-3}N·m^{-1})	dγ/dT (10^{-3}N·m^{-1}K^{-1})	Temperature (K)	Reference
Hf	1614	-0.10	2220-2670	Present work[47]
	1630		2504	Allen[30]
2504	1460		2504	Peterson[36]
	1490		2504	Kostikov[61]

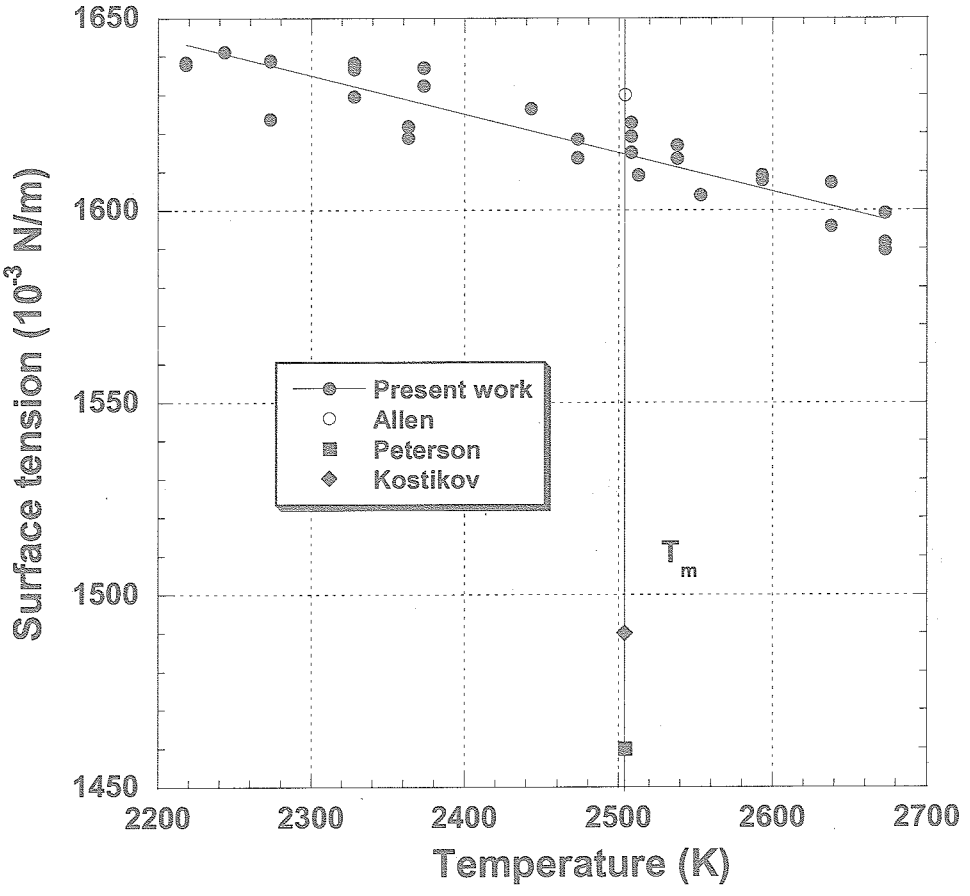

Fig.19 Surface tension of liquid hafnium versus temperature.

Table 17 Literature values of the surface tension for tantalum

Metal T_m (K)	$\gamma(T_m)$ (10^{-3}N·m^{-1})	$d\gamma/dT$ (10^{-3}N·m^{-1}K^{-1})	Temperature (K)	Reference
Ta	2154	-0.21	3143-3393	Present work[68]
	2150		3290	Allen[30]
3290	1910		3290	Namba [69]
	2016		3290	Eremenko[65]
	2360		3290	Kelly [70]
	2030		3290	

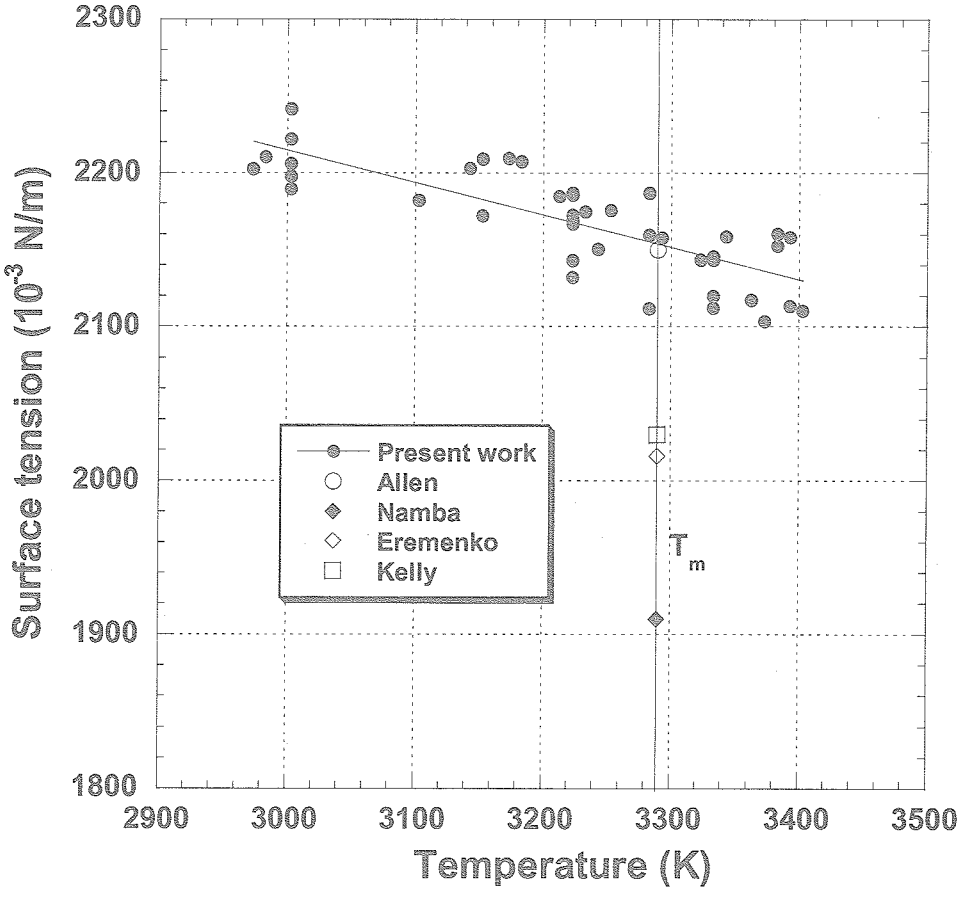

Fig.20 Surface tension of liquid tantalum versus temperature.

Table 18 Literature values of the surface tension for tungsten

Metal T_m (K)	γ (T_m) (10^{-3}N·m^{-1})	dγ/dT (10^{-3}N·m^{-1}K^{-1})	Temperature (K)	Reference
W	2477	-0.31	3398-3693	Present work[52]
	2300		3693	Calverley[53]
3695	2500		3693	Allen[30]
	2200		3693	Pekarev[40]
	2316		3693	Martsenyuk[71]
	2300		3693	Agaev[72]

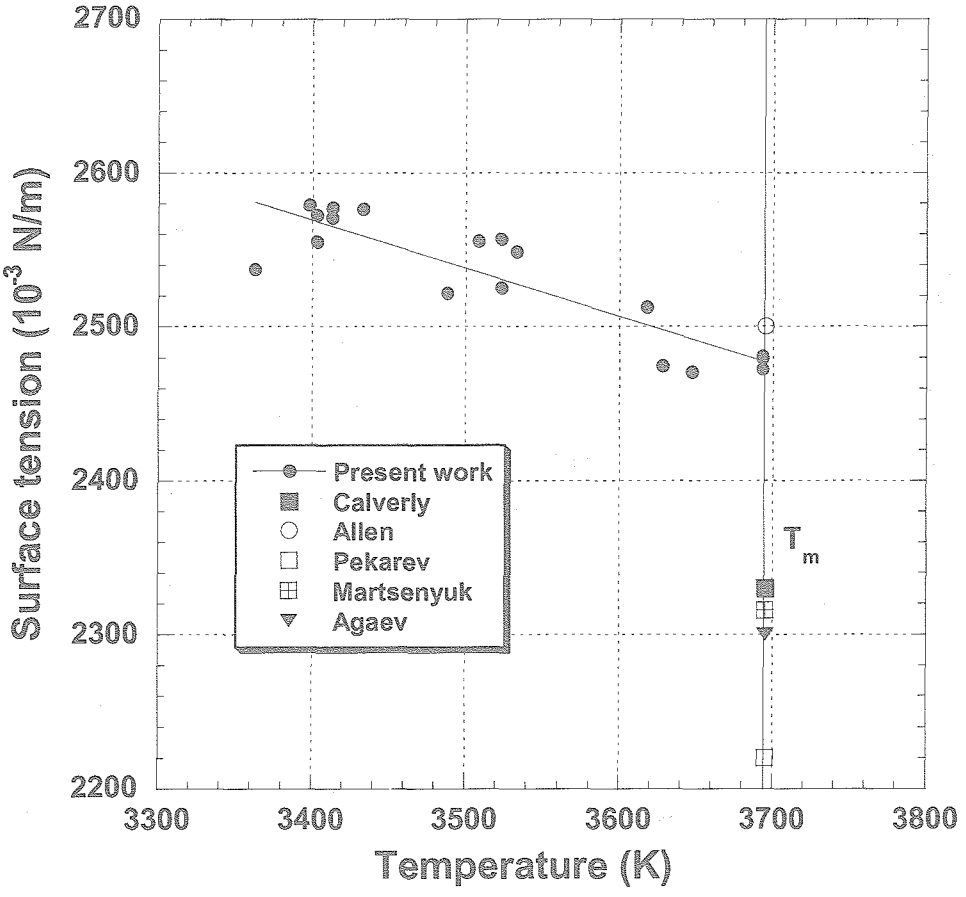

Fig.21 Surface tension of liquid tungsten versus temperature.

Table 19 Literature values of the surface tension for rhenium

Metal T_m (K)	γ (T_m) (10^{-3}N·m^{-1})	dγ/dT (10^{-3}N·m^{-1}K^{-1})	Temperature (K)	Reference
Re 3459	2710	-0.23	2903-3583	Present work[73]
	2700		3459	Allen[30]
	2610		3459	Pekarev[40]

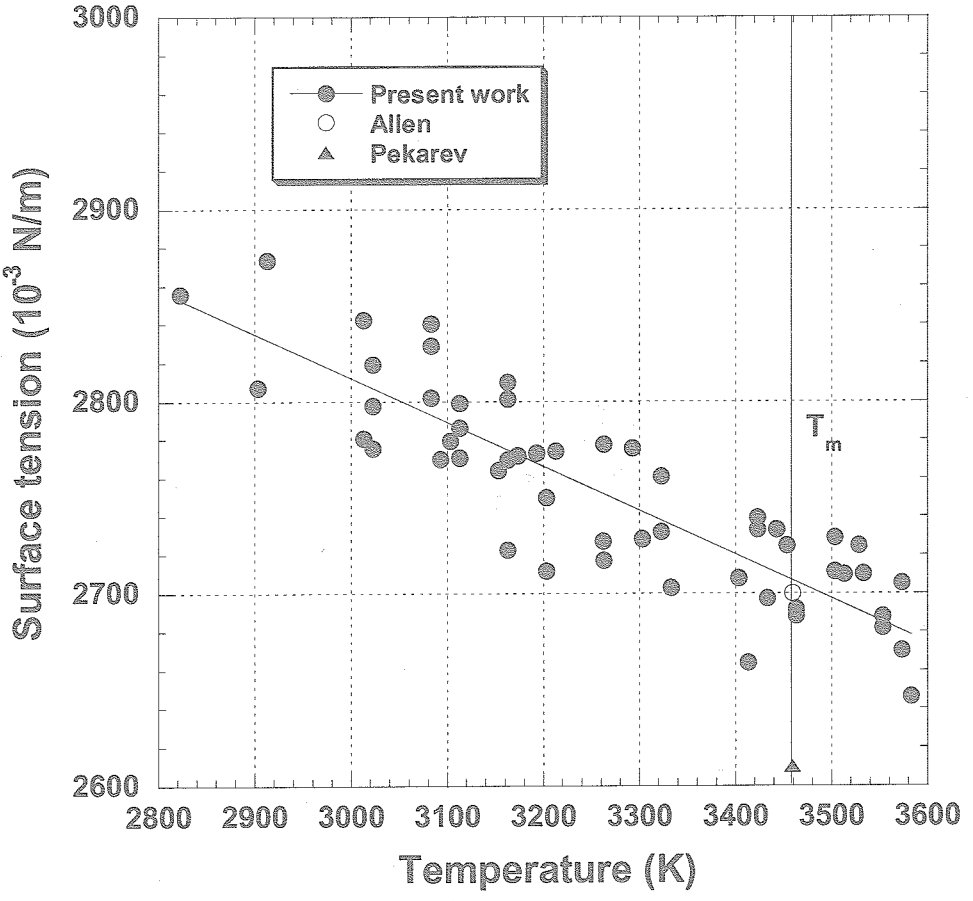

Fig.22 Surface tension of liquid rhenium versus temperature.

Table 20 Literature values of the surface tension for iridium

Metal T_m (K)	γ (T_m) (10^{-3}N·m^{-1})	Temp. Coeff. (10^{-3}N·m^{-1}K^{-1})	Temperature (K)	Reference
Ir	2241	-0.16	2373-2833	Present work[55]
	2250		2720	Allen[40]
2719	2264	-0.247	2720-	Apollova[74]
	2140		2720	Martensyuk[75]

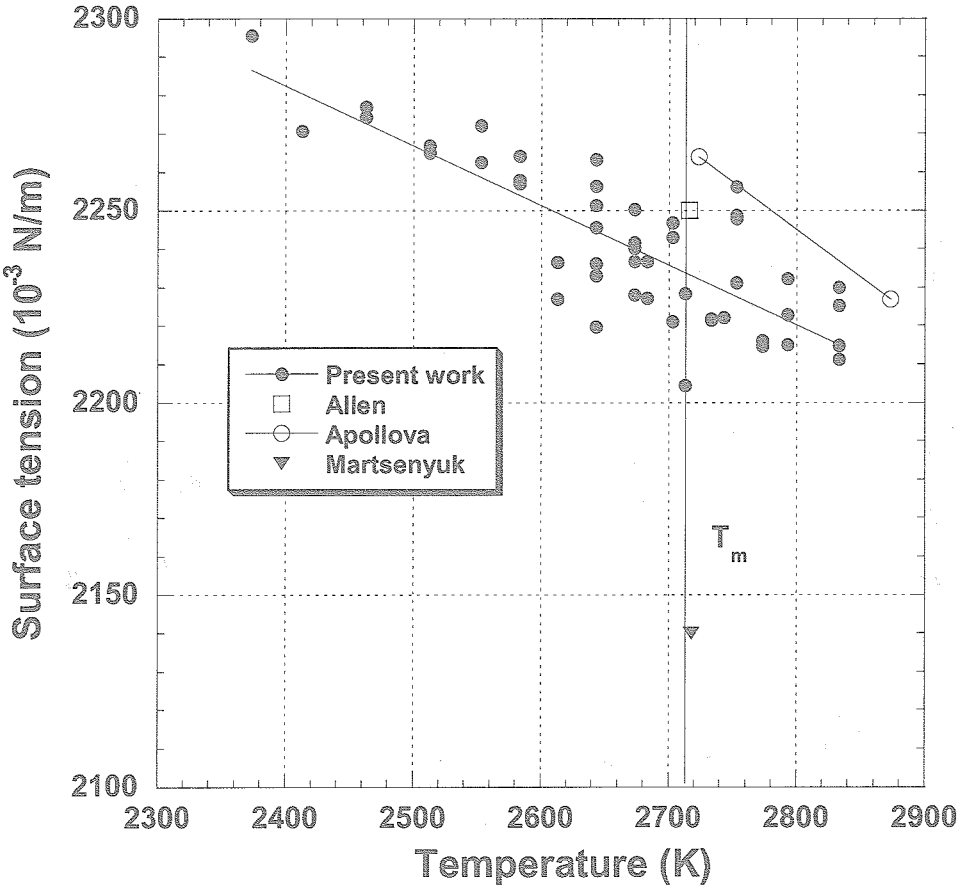

Fig.23 Surface tension of liquid iridium versus temperature.

4. 3. Viscosity

Table-21 to 29 and **Fig.24** to **32** show the viscosity data for refractory metals. To our knowledge, viscosity data of niobium, ruthenium, tantalum, rhenium, tungsten and iridium were the first to be reported. The uncertainty of viscosity was estimated to be around 15%. This relatively large uncertainty is mainly caused by sample motion during drop oscillation that generates extra noise on the decay signal that lead to large uncertainty in τ. Surface tension and viscosity measurements for molybdenum, tantalum, and rhenium are currently being conducted and will be presented in a later publication.

Table 21 Literature values of the viscosity for zirconium

Metal T_m (K)	η (T_m) (10^{-3}Pa·s)	$\eta(T)=\eta_0 \cdot \exp(E/RT)$		Temperature (K)	Reference
		η_0 (10^{-3}Pa·s)	E (10^3J·mol^{-1})		
Zr	4.7	0.76	31.8	1800-2300	Present work[59]
	4.83			1850-2200	Paradis[7]
2128	3.5			2133	Agaev[76]
	5.45			2138	Elyutin[77]

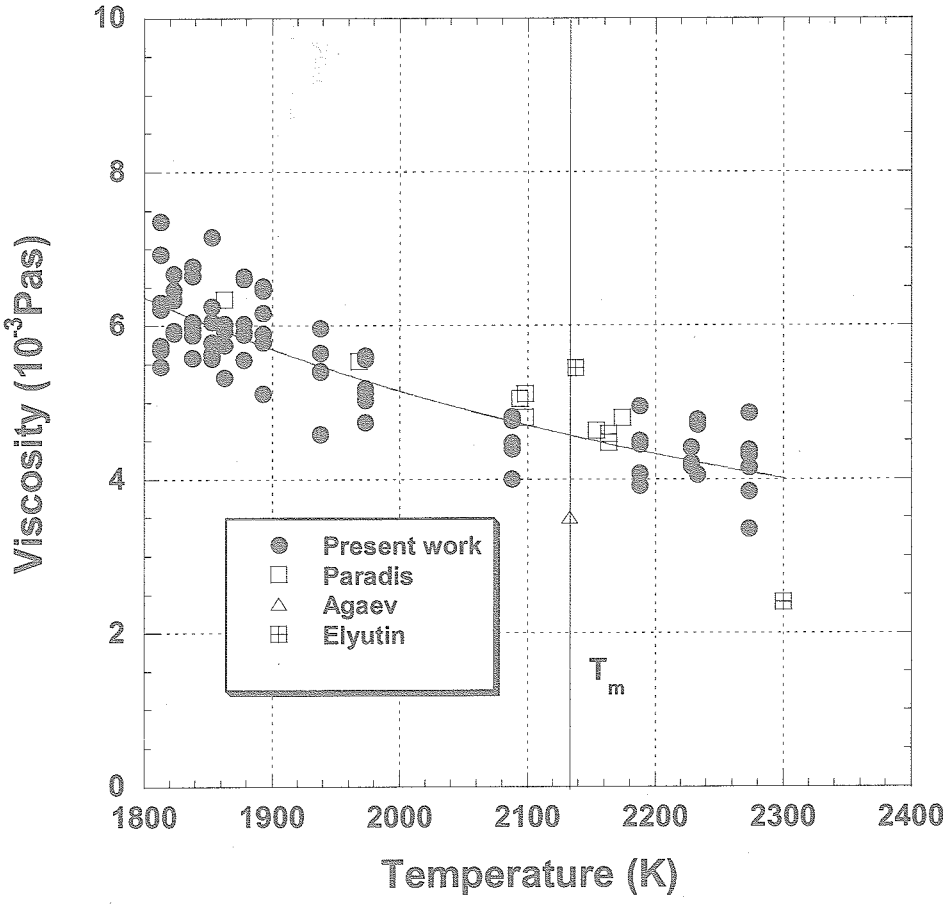

Fig.24 Viscosity of liquid zirconium versus temperature.

Table 22 Literature values of the viscosity for niobium

Metal T_m (K)	η (T_m) (10^{-3}Pa·s)	$\eta(T)=\eta_0 \cdot \exp(E/RT)$		Temperature (K)	Reference
		η_0 (10^{-3}Pa·s)	E (10^3J·mol^{-1})		
Nb 2742	4.5	0.55	48.9	2320-2915	Present work[59]

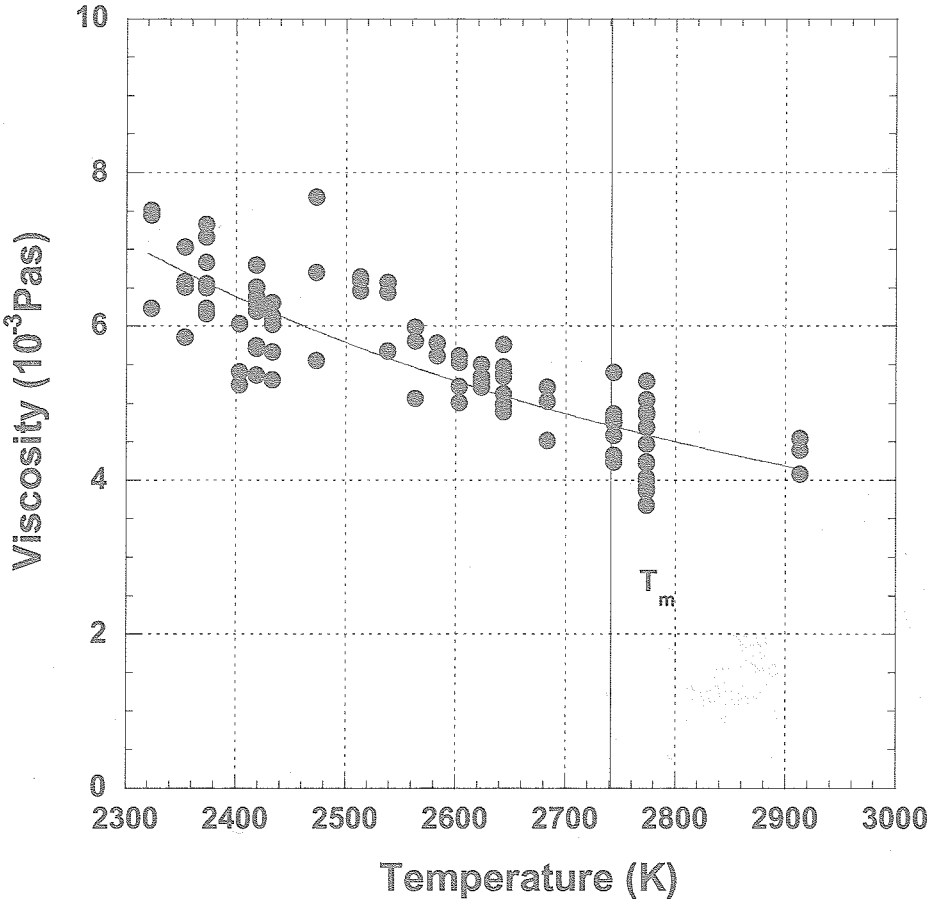

Fig.25 Viscosity of liquid niobium versus temperature

Table 23 Literature values of the viscosity for ruthenium

Metal T_m (K)	η (T_m) (10^{-3}Pa·s)	$\eta(T)=\eta_0 \cdot \exp(E/RT)$		Temperature (K)	Reference
		η_0 (10^{-3}Pa·s)	E (10^3J·mol^{-1})		
Ru 2607	6.1	0.60	49.8	2450-2725	Present work[41]

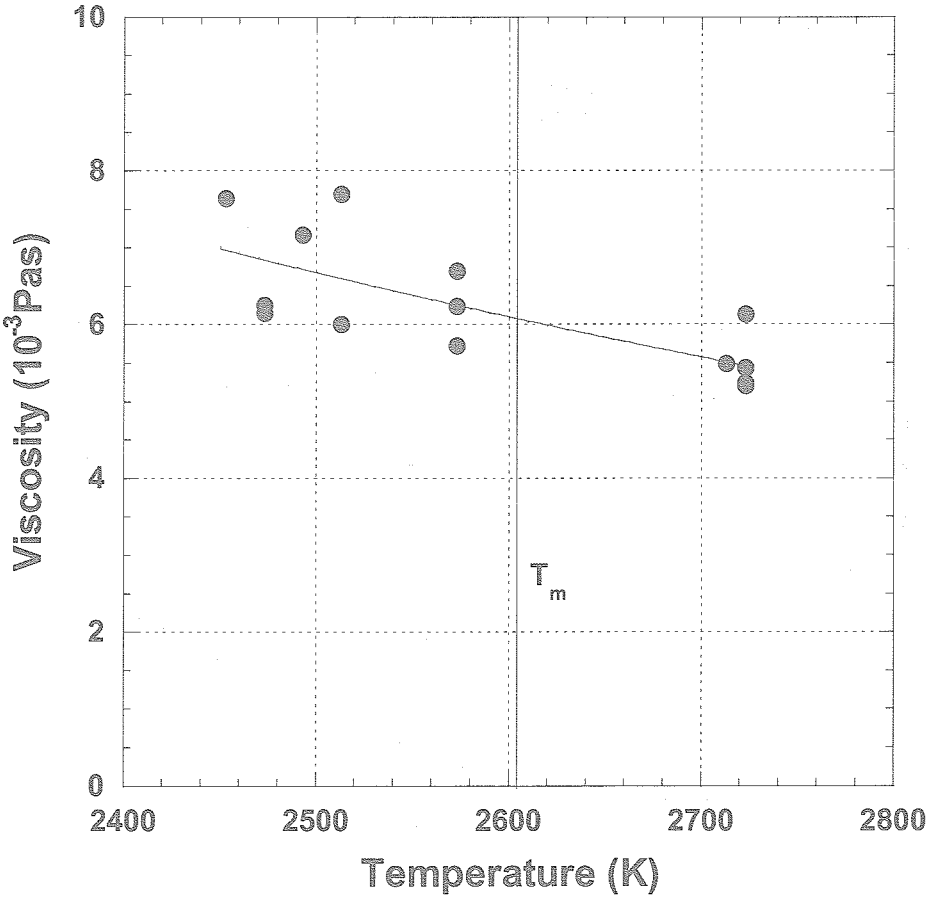

Fig.26 Viscosity of liquid ruthenium versus temperature.

Table 24 Literature values of the viscosity for rhodium

Metal T_m (K)	η (T_m) (10^{-3}Pa·s)	$\eta(T)=\eta_0 \cdot \exp(E/RT)$		Temperature (K)	Reference
		η_0 (10^{-3}Pa·s)	E (10^3J·mol^{-1})		
Rh 2236	2.9	0.09	64.3	1860-2380	Present work[42]
	5			2236	Demidovich[78]

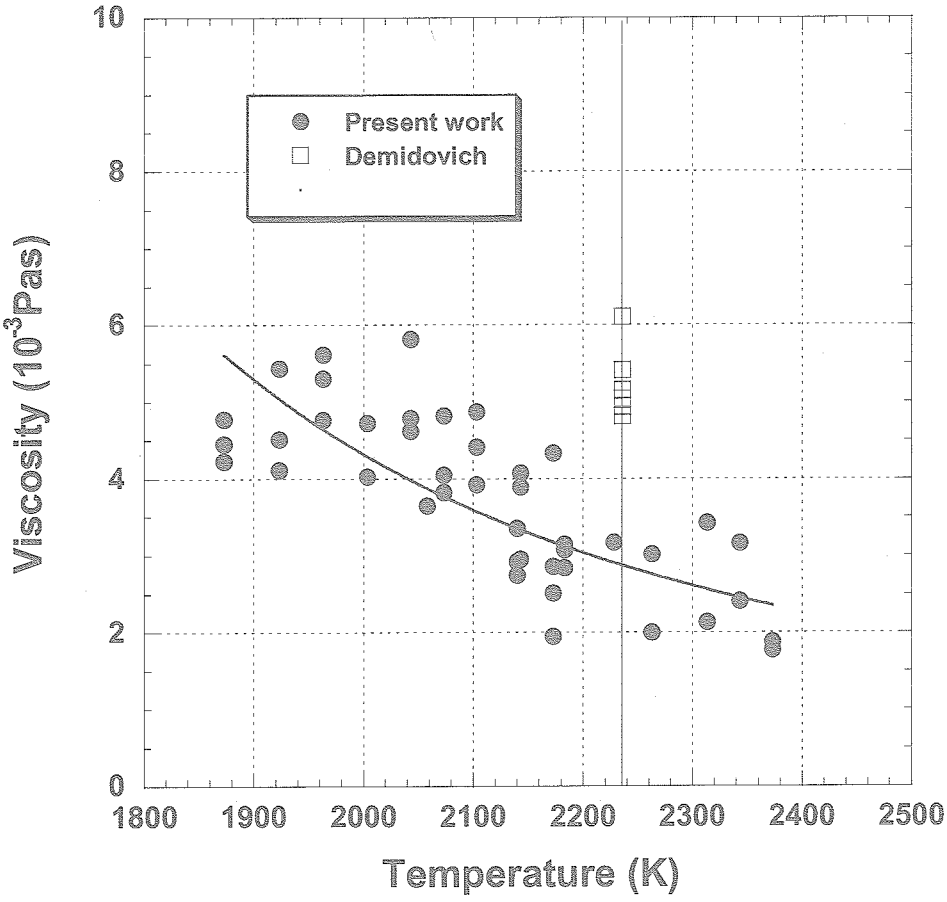

Fig.27 Viscosity of liquid rhodium versus temperature.

Table 25 Literature values of the viscosity for hafnium

Metal T_m (K)	η (T_m) (10^{-3}Pa·s)	$\eta(T)=\eta_0 \cdot \exp(E/RT)$		Temperature (K)	Reference
		η_0 (10^{-3}Pa·s)	E (10^3J·mol^{-1})		
Hf 2504	5.2	0.50	48.7	2220-2670	Present work[47]
	5.0			2504	Agaev[76]

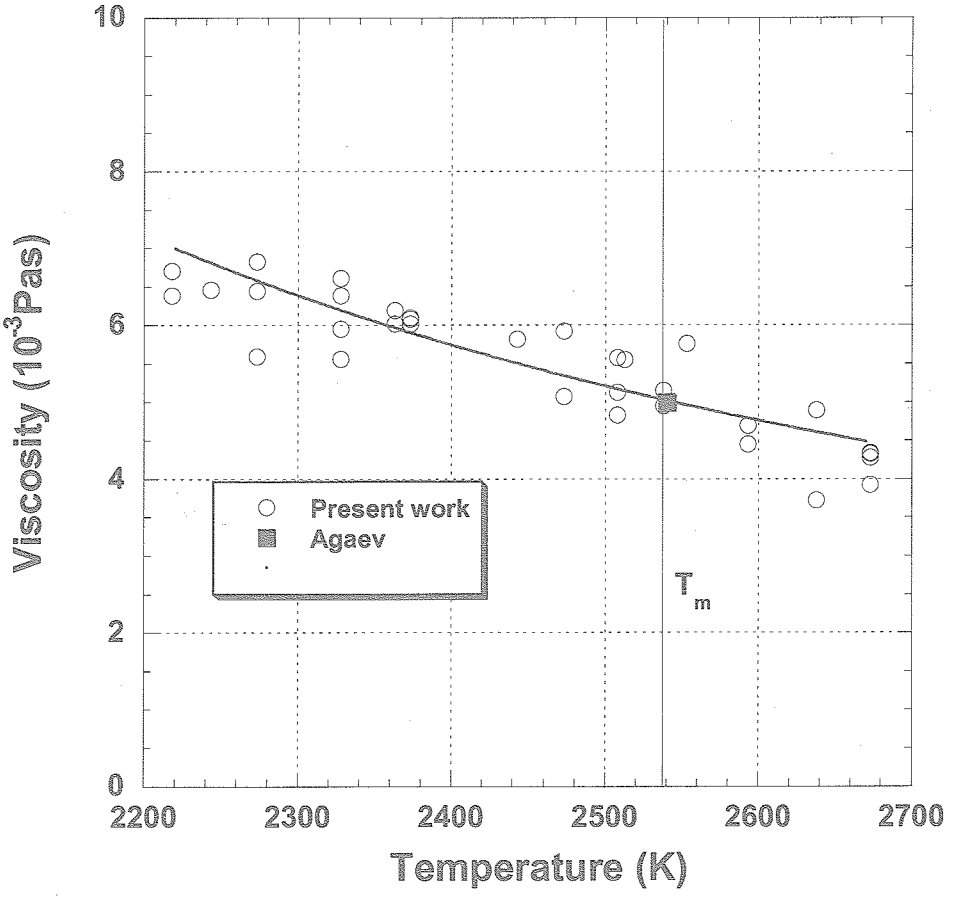

Fig.28 Viscosity of liquid hafnium versus temperature.

Table 26 Literature values of the viscosity for tantalum

Metal T_m (K)	η (T_m) (10^{-3}Pa·s)	$\eta(T)=\eta_0 \cdot \exp(E/RT)$		Temperature (K)	Reference
		η_0 (10^{-3}Pa·s)	E (10^3J·mol^{-1})		
Ta 3290	8.6	0.004	213	3143-3393	Present work[68]

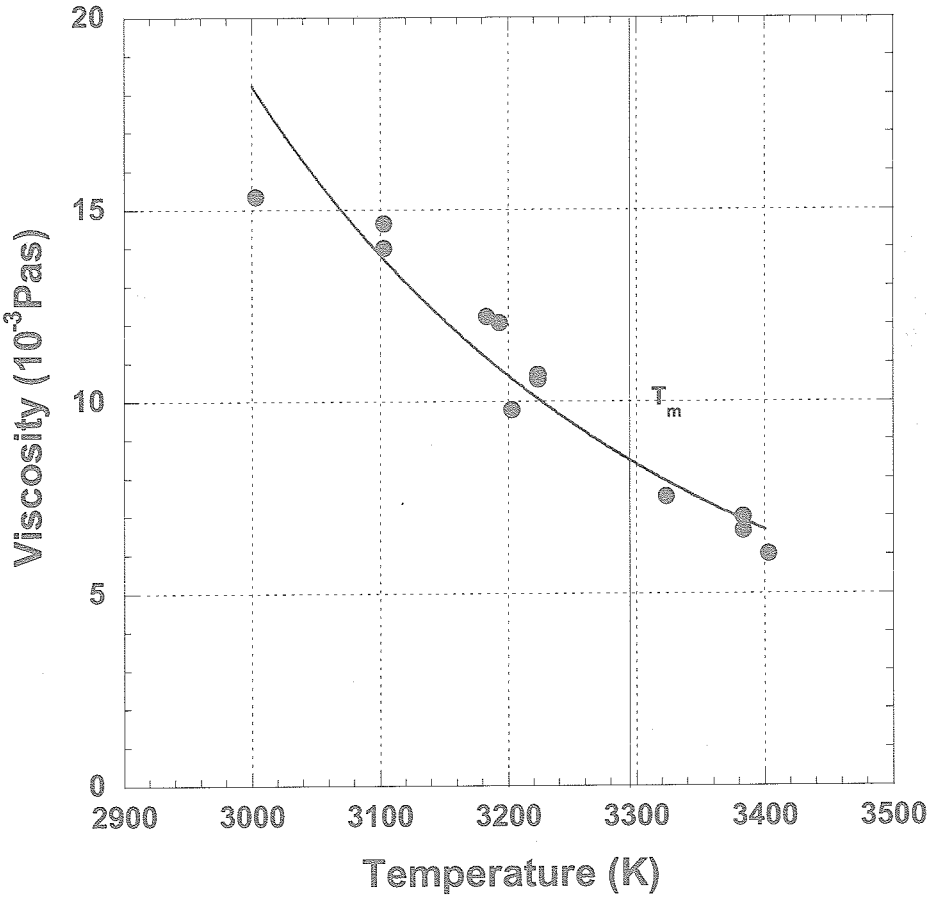

Fig.29 Viscosity of liquid tantalum versus temperature.

Table 27 Literature values of the viscosity for tungsten

Metal T_m (K)	η (T_m) (10^{-3}Pa·s)	$\eta(T)=\eta_0 \cdot \exp(E/RT)$		Temperature (K)	Reference
		η_0 (10^{-3}Pa·s)	E (10^3J·mol^{-1})		
W 3695	6.9	0.11	128	3398-3693	Present work[79]

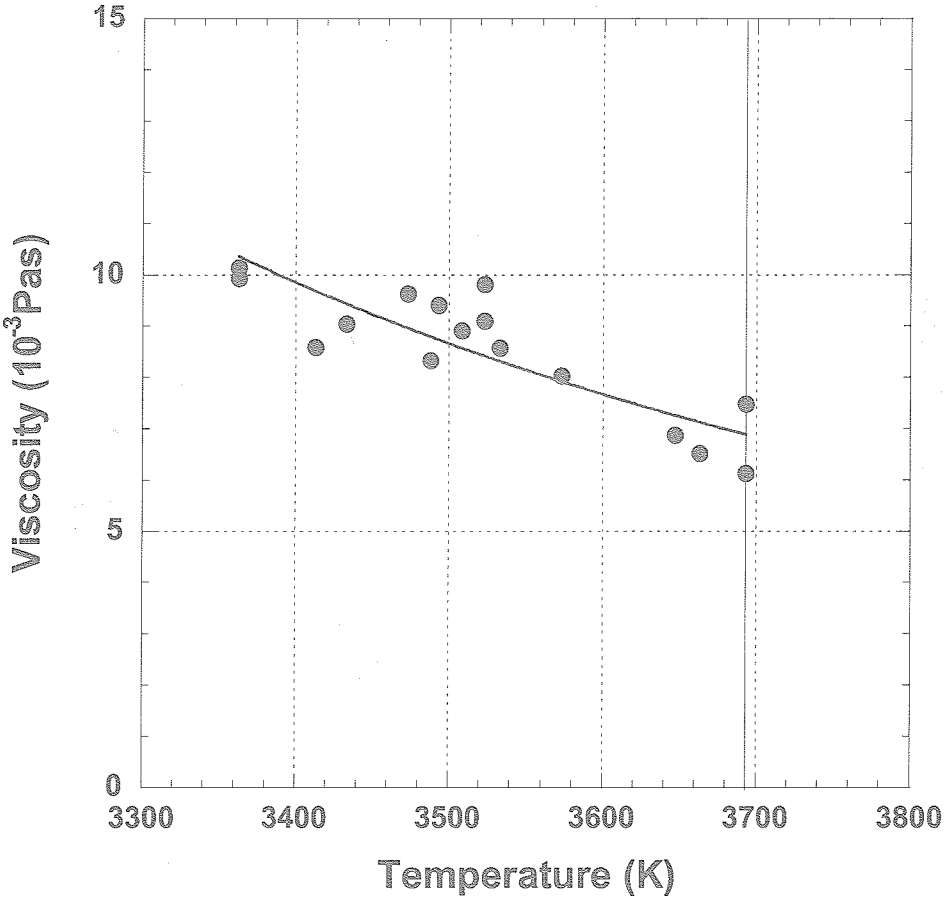

Fig.30 Viscosity of liquid tungsten versus temperature.

Table 28 Literature values of the viscosity for rhenium

Metal T_m (K)	η (T_m) (10^{-3}Pa·s)	$\eta(T)=\eta_0 \cdot \exp(E/RT)$		Temperature (K)	Reference
		η_0 (10^{-3}Pa·s)	E (10^3J·mol^{-1})		
Re 3459	7.9	0.08	133	2903-3583	Present work[73]

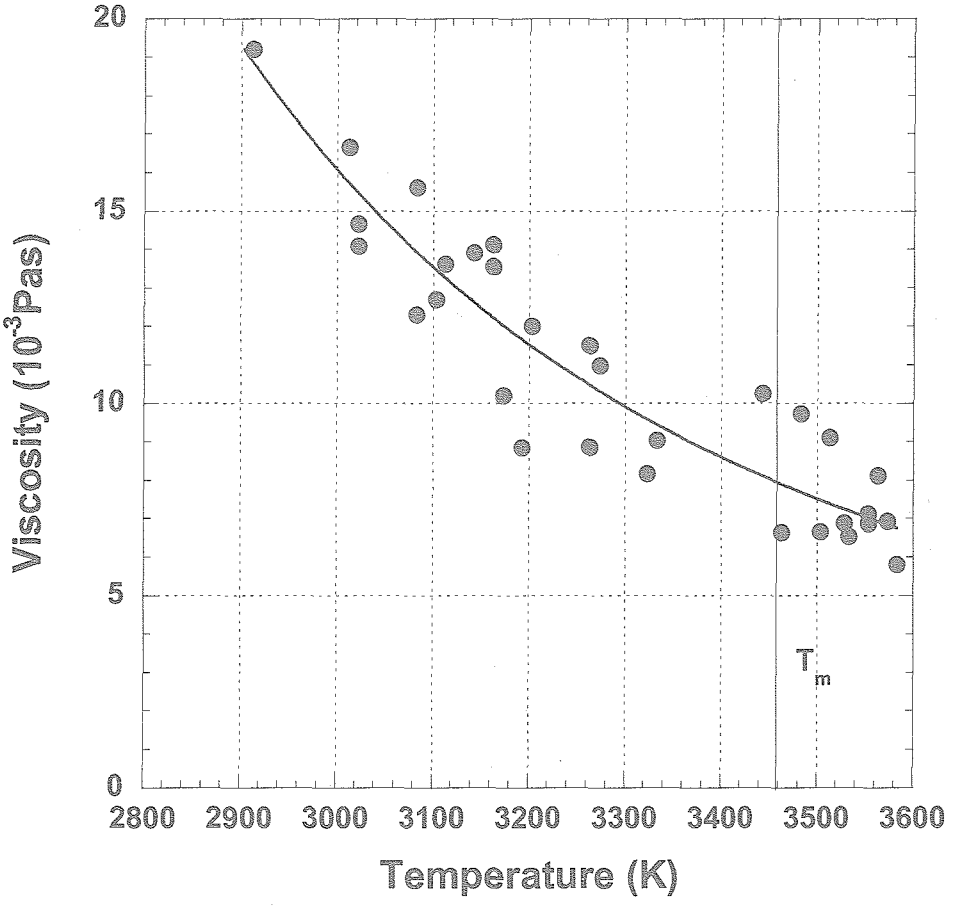

Fig.31 Viscosity of liquid rhenium versus temperature.

Table 29 Literature values of the viscosity for iridium

Metal T_m (K)	η (T_m) (10^{-3}Pa·s)	$\eta(T)=\eta_0 \cdot \exp(E/RT)$		Temperature (K)	Reference
		η_0 (10^{-3}Pa·s)	E (10^3J·mol^{-1})		
Ir 2719	7.0	1.85	30.0	2373-2773	Present work[55]

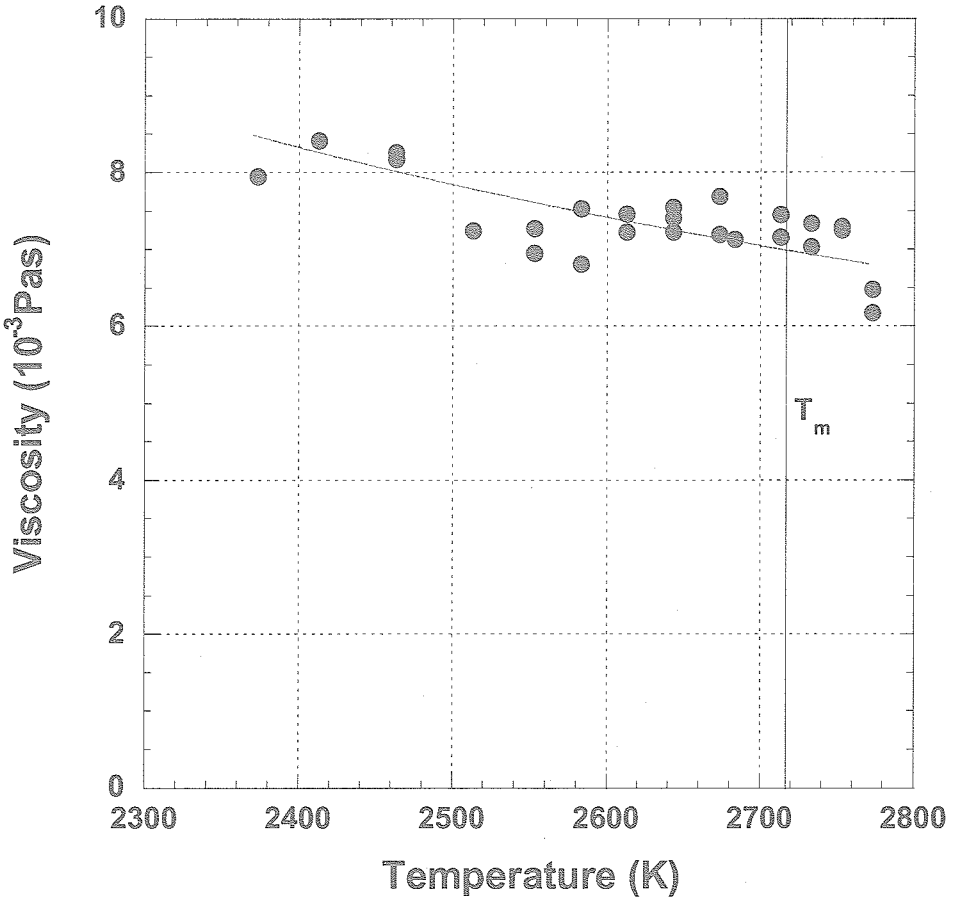

Fig.32 Viscosity of liquid iridium versus temperature.

4. 4 Comparison between hard sphere model calculations

One of our research interests on measuring thermophysical properties of refractory metals is to find relations between the microscopic structure and macroscopic (thermophysical) properties in liquid transition metals. Compared to simple liquid metals such as alkaline metals, which consist of s and p valence electrons, liquid transition metals are partially filled with d bands electrons and more complicated. Due to the presence of these d electrons, successful prediction could hardly be done for liquid transition metals.[80] Furthermore, lack of reliable thermophysical properties of refractory metals prevented the progress of theoretical research.

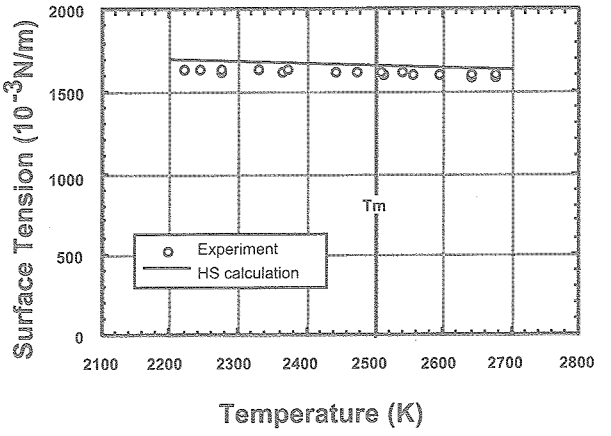

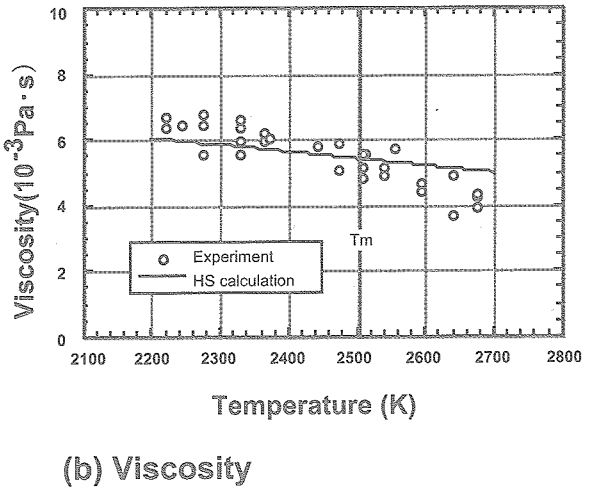

Fig.33 Measured and calculated thermophysical properties of hafnium: (a)surface tension and (b) viscosity.

Fig. 33 shows the comparison between our measured data of hafnium and calculated values based on the modified hard sphere model.[81] Despite of the simplicity of the model, agreement between measured data and calculated values is good and proved the reliability of the non-contact thermophysical property measurements with the ELF.

Containerless techniques are also powerful tools to study microscopic structure of liquid refractory metals. Pioneering works have already been done by coupling x-ray diffraction with aerodynamic levitator[82] and EXAFS with an electromagnetic levitator.[83] Shenk et al. investigated the atomic structure of liquid nickel, iron, and

zirconium over wide temperature ranges using the combination of electromagnetic levitation with neutron scattering.[84] Kelton et al. combined an electrostatic levitator with synchrotron and measured the structure of liquid Ti-Ni-Zr alloy.[85] Knowledge of structure and thermophysical properties of liquid refractory metals determined by containerless methods will promote theoretical research.

5. Necessity of microgravity condition

Although several successes were achieved over the years on the ground with ELFs (high vacuum and pressurized), difficulties are faced when handling platinum, iron, certain alloys, and oxides due to insufficient sample charges before reaching the melting temperature or sudden charge loss at melting, leading to an interruption in levitation. Microgravity conditions would allow easier non-contact positioning of these metals or larger samples while providing a quiet environment.

For surface tension measurement, sample deformation due to gravity is taken into consideration in equation (2). Surface tension measurements in microgravity condition is necessary to check the validity of equation (2), which has been derived from theoretical analysis.

Microgravity condition is more important for viscosity measurement. More stable sample positioning could be achieved in microgravity, which would result in lesser noise on oscillation decay signal. Furthermore, because levitation or positioning force could have same effects on the oscillation damping, measurement in microgravity, where positioning force can be minimized, is ideal for viscosity measurement by the oscillation drop technique.

6. Conclusions

Thermophysical properties of several refractory metals over wide temperature ranges in the undercooled as well as in the superheated state could be measured using the unique capabilities of the electrostatic levitation furnace. On-going efforts focus on tungsten, whose melting temperature is the highest among metals. Containerless processing facilities are powerful tools for thermophysical property measurements of high temperature materials not only on the ground but also in microgravity. The ISS version of the ELF will be designed and developed based on the results of this ground-based facility.

7. Acknowledgment

Authors would like to express their gratitude to Dr. J. Yu, Dr. T. Aoyama, and Mr. Y. Saita (Advanced Engineering Service Co. Ltd.) for help in some experiments. This work was partially supported by a Grant-in-Aid for Science Research (B) from the Japan Society for the Promotion of Science.

References

[1] I. Egry, A. Diefenbach, W. Dreier, and J. Piller, "Containerless Processing in Space – Thermophysical Property Measurements Using Electromagnetic Levitation", *Int. J. of Thermophysics*, **22** (2001), 569-578.

[2] R. K. Wunderlich, Ch. Ettl, and H. –J. Fecht, "Spacific Heat and Thermal Transport Measurements of Reactive Metallic Alloys by Noncontact Calorimetry in Reduced Gravity", *Int. J. of Thermophysics*, **22** (2001), 579-591.

[3] G. Lohofer, S. Schneider, and I. Egry, "Thermophysical Properties of Undercooled Liquid $Co_{80}Pd_{20}$", *Int. J. of Thermophysics*, **22** (2001), 593-604.

[4] P. F. Clancy, E. G. Lierke, R. Grossbach, and W. M. Heide, "Electrostatic and acoustic instrumentation for material science

processing in space", *Acta Astronautica*, **7** (1980), 877-891.

[*5*] E. G. Lierke, R. Grossbach, G. H. Frischat, K. Fecker, "Electrostatic positioning for the containerless processing of a Li-silicate glass", in Suumary Review of Sounding Rocket Experiments in Fluid Science and Materials Sciences, esa **SP-1132** (1991), 370-371.

[*6*] W.-K. Rhim, S. K. Chang, D. Barber, K. F. Man, G. Gutt, A. Rulison, and R. E. Spjut, "An electrostatic levitator for high-temperatuer containerless materials processing in 1-g" *Rev. Sci. Instrum.*, **64** (1993), 2961-2970.

[*7*] P. -F. Paradis and W. K. Rhim, "Thermophysical properties of zirconium at high temperature", *J. Mater. Res.*, **14** (1999), 3713-3719.

[*8*] P. -F. Paradis and W. K. Rhim, "Non-contact measurements of thermophysical properties of titanium at high temperature", *J. Chem. Thermodyn.*, **32** (2000), 123-133.

[*9*] W. K. Rhim, S. K. Chung, A. J. Rulison, and R. E. Spjut, "Measurements of Thermophysical Properties of Molten Silicon by a High-Temperature Electrostatic Levitator", *Int. J. of Thermophysics*, **18** (1997), 459-469.

[*10*] W. -K. Rhim and T. Ishikawa, "Thermophysical Properties of Molten Germanium Measured by a High-Temperature Electrostatic Levitator", *Int. J. of Thermophysics*, **21** (2000), 429-443.

[*11*] S. K. Chung, D. B. Thiessen, and W. K. Rhim, "A noncontact measurement technique for the density and thermal expansion coefficient of solid and liquid materials", *Rev. Sci. Instrum.*, **67** (1996), 3175-3181.

[*12*] A. J. Ruliuson and W. K. Rhim, "A noncontact measurement technique for the specific heat and total hemispherical emissivity of undercooled refractory materials", *Rev. Sci. Instrum.*, **65** (1994), 695-700.

[*13*] W. K. Rhim, K. Ohsaka, and P. -F. Paradis, "Noncontact technique for measuring surface tension and viscosity of molten materials using high temperature electrostatic levitation", *Rev. Sci. Instrum.*, **70** (1999), 2796-2799.

[*14*] W. -K. Rhim and T. Ishikawa, "Noncontact electrical resistivity measurement technique for molten metals", *Rev. Sci. Instrum.*, **69** (1998), 3628-3633.

[*15*] M. B. Robinson, D. Li, J. R. Rogers, R. W. Hyers, L. Savage, and T. J. Rathz, "High undercooling of $Ni_{59}Nb_{41}$ Alloy in a containerless electrostatic levitation facility", *Appl. Phys. Lett.*, 77 (2000), 3266-3268.

[*16*] A. J. Rulison, J. L. Watkins, and B. Zambrano, "Electrostatic containerless processing system", *Rev. Sci. Instrum.*, **68** (1997), 2856-2863.

[*17*] T. Meister, H. Werner, G. Lohoefer, D. M. Herlach, and H. Unbehauen, "Gain-scheduled control of an electrostatic levitator", *Control Engineering Practice*, **11** (2003), 117-128.

[*18*] T. Ishikawa, P.-F. Paradis, and S. Yoda, "Development of Ground-based Electrostatic Levitation Furnace", *J of Jpn Soc. of Microgravity Appl.* **18** (2001), 106-115.

[*19*] J. Yu, N. Koshikawa, Y. Arai, and S. Yoda, H. Saito," Containerless solidification of oxide material using an electrostatic levitation furnace in microgravity", *J. Cryst. Growth,* **231** (2001) 568-576.

[*20*] P.-F. Paradis, T. Ishikawa, S. Yoda, " Position stability analysis of electrostatically levitated samples for thermophysical and structural properties measurements of materials", *Space Technol.* **22** (2002), 81-92.

[*21*] P. -F. Paradis, T. Ishikawa, S. Yoda, "Hybrid electrostatic-aerodynamic levitation furnace for the high temperature processing of oxide materials on the ground", *Rev. Sci. Instrum.*, **72** (2001), 2811-2815.

[*22*] P. -F. Paradis, J. Yu, T. Ishikawa, T. Aoyama, S. Yoda, and J. K. R. Weber, "Contactless density measurement of superheated and undercooled liquid $Y_3Al_5O_{12}$", *J. Cryst. Growth,* **249** (2003), 523-530.

[*23*] P. -F. Paradis, J. Yu, T. Ishikawa, T. Aoyama, and S. Yoda, "Contactless density measurement of liquid and high temperature solid $BiFeO_3$ and $BaTiO_3$", *Applied Phys. A* **76** (2003),1-5.

[*24*] P. -F. Paradis, J. Yu, T. Aoyama, T. Ishikawa, S. Yoda, "Contactless density measurement of liquid Nd-doped 50%CaO-

50%Al_2O_3", *J. Am. Ceram. Soc.*, **86** (2003), 2234-2236.

[*25*] T. Ishikawa, P. -F. Paradis, S. Yoda, "New sample levitation initiation and imaging techniques for the processing of refractory metals with an electrostatic levitator furnace", *Rev. Sci. Instrum.*, **72** (2001), 2490-2495.

[*26*] P. M. Adornato and R. A. Brown, "Shape and stability of electrostatically levitated drops", *Proc. R. Soc. Lond.*, **A389** (1983), 101-107.

[*27*] W. –K. Rhim, S. K. Chung, and D. D. Elleman, "Electrostatic levitators and drop dynamics experiments", *Proc. 7th european symposium on materials and fluid science in microgravity*, Oxford, UK, **ESA SP-295** (1990), 629-637.

[*28*] H. Lamb, *Hydrodynamics*, 6th ed. (Cambridge University Press, Cambridge, 1932), 473.

[*29*] P.-F. Paradis, T. Ishikawa, T. Aoyama, S. Yoda, "Thermophysical properties of vanadium at high temperature measured by an electrostatic levitation furnace", *J. Chem. Thermodyn.*, **34** (2002), 1929-1942.

[*30*] B.C. Allen, "The surface tension of liquid transition metals at their melting points", *Trans. AIME* **227**, (1963), 1175-1183.

[*31*] M. A. Maurakh, "Surface tension of titanium, zirconium, and vanadium", *Trans. Indian Inst. Metals*,(1961), 205-225.

[*32*] T. Saito, Y. Shiraishi, and Y. Sakuma, "Density Measurement of Molten Metals by Levitation Technique at Temperature between 1800 and 2200 C", *Trans. Iron and Steel Inst. Japan*, **9**(1969), 118-126.

[*33*] V. P. Eljutin, V. I. Kostikov, and I. A. Penkov, "Hydrogen effect on the surface strain and compactness of liquid vanadium, niobium and molybdenum", *Poroshk. Met.*, **9** (1970), 46-5.

[*34*] U. Seydel and W. Kitzel, "Thermal volume expansion of liquid Ti, V, Mo, Pd, and W", *J. Phys. F: Metal Phys.*, **9** (1979), L153-160.

[*35*] T. Ishikawa, P. –F. Paradis, and S. Yoda, "Thermophysical Property measurements of refractory metals using a ground-based electrostatic levitation furnace", *Proc. of 2nd Pan Pacific Basin Workshop on Microgravity Sciences*, Pasadena, (2001),TP-1019.

[*36*] A. W. Peterson, H. Kadesky, P. H. Keck, and E. Scharz, "Surface Tension of Titanium, Zirconium, and Hafnium", *J. Appl. Phys.*, **29**(1958), 213.

[*37*] Yu. N. Ivashchenko and P. S. Martsenyuk, *High Temp.*, **11** (1973), 1146.

[*38*] J. W. Shaner, G. R. Gathers, C. Minichino, "A new apparatus for thermophysical measurements above 2500K", *High temp. -High Press.* **8** (1976), 425-429.

[*39*] P.-F. Paradis, T. Ishikawa, S. Yoda, "Non-contact measurements of thermophysical properties of molybdenum at high temperature", *Int. J. of Thermophysics,* **23**(2002), 555-569.

[*40*] V. Pekarev, *Izv. Vyss. Uch. Sav., Tsvetn. Met.*, **6** (1963), 111.

[*41*] P. -F. Paradis, T. Ishikawa, and S. Yoda, "Thermophysical Properties of liquid and supercooled ruthenium measured by noncontact methods", *J. Mater. Res,* **19**(2004), 590-594.

[*42*] P. -F. Paradis, T. Ishikawa, and S. Yoda, "Thermophysical Property Measurements of Supercooled and Liquid Rhodium", *Int. J. of Thermophysics*, **24** (2003), 1121-1136.

[*43*] V. N. Eremenko and Yu. V. Naidich, *Izv. Akad. Nauk. SSR, O. T. N. Met. Topliva*, **6** (1961), 100.

[*44*] M. M. Mitko, E. L. Dubinin, A. I. Timofejev, and L. I. Chegodajev, *Izv. Vyss. Uchebn. Saved., Tsvetn. Met.*, **3** (1978),84.

[*45*] S. I. Popel, B. V. Tsareveskii, and N. K. Dzhemilev, *Fiz. Met. Metall. SSSR*, **18** (1964), 468.

[*46*] E. L. Dubinin, V. M. Vlasov, A. I. Timofejev, S. O. Safonov, and A. I. Chegodajev, *Izv. Vtss. Uchebn. Saved., Tsvetn,* Met., **4** (1975), 160.

[*47*] P. -F. Paradis, T. Ishikawa, S. Yoda, "Non-contact measurements of thermophysical properties of hafnium-3%(Wt) zirconium at high temperature", *Int. J. of Thermophysics*, **24** (2003), 239-258.

[*48*] Yu N. I. Ivashcheko and P. S. Martsenyuk, *Zavod. Lab.* **39** (1973), 42.

[*49*] V. I. Arkhipkin, G. A. Grigoriev and V. I. Kostikov, Fiz. Khim. Granits Razdeia kontaktiryuschikh Faz. (1976), p74-77, edited by

V. N. Eremenko, Naukova Dumka-Kiev USSR.

[50] P. -F. Paradis, T. Ishikawa, and S. Yoda, "Noncontact density measurements of tantalum and rhenium in the liquid and undercooled states", *Appl. Phys. Lett.*, **83**(2003), 4047-4049.

[51] A. Berhault, L. Arles, and J. Matricon, "High-Pressure, High-Temperature Thremophysical Measurements on Tantalum and Tungsten", *Int. J. of Thermophysics*, 7(1986), 167.

[52] P. -F. Paradis, T. Ishikawa, R. Fujii, and S. Yoda, "Physical Properties of Liquid and Undercooled Tungsten by Levitation Techniques", in press, *Appl. Phys. Lett.*

[53] A.Calverley, "A determination of the surface tension of liquid tungsten by the drop-weight method", *Proc. Phys. Soc.*, **70** (1957), 1040.

[54] T. Thevenin, L. Alres, M. Boivineau, J. M. Vermeulen, *Int. J. of Thermophysics,* **14** (1993), 441.

[55] T. Ishikawa, P. -F. Paradis, and S. Yoda, "Thermophysical property measurements of liquid and supercooled iridium by containerless methods", in press, *Int. J. of Thermophysics.*

[56] P. S. Martensyuk and Yu N. I. Ivaschtschenko, *Ukr. Chim. Sh.*, **40**(1974),431.

[57] T. A. Apollova, E. L. Dubinin, M. M .Mitko, A. I. Chegodayev, and L .L. Bezuladnkova, *Izv. A.N., SSSR, Met.*, **6** (1982), 55.

[58] G. R. Gathers, J. W. Shaner, R. S. Hixson, and D. A. Jung, *High-Temp High-Press*, **11** (1979), 653

[59] P. -F. Paradis, T. Ishikawa and S. Yoda, "Non-contact Measurements of Surface Tension and Viscosity of Niobium, Zirconium and Titanium Using an Electrostatic Levitation Furnace", *Int. J. of Thermophysics*, **23**(2002), 825-842.

[60] R. Shunk and M. Burr, *Trans. AIME*, **55** (1962), 786.

[61] V. I. Kostikov, B. D. Grigorjev, P. G. Arkhipkin, and A. D. Agaev, *Izv. Vyss. Uch. Sav. Chern. Met.*, **3** (1972), 25.

[62] O. Flint, *J. Nucl. Mat.*, **16** (1965), 260.

[63] Yu. N. Ivaschenko, and P. C. Marchenuk, *Teplov. Vys. Temp.*, **11** (1973), 1285-1287.

[64] V. I. Arkhipkin, A. D. Agaev, G. A. Grigorev, and V. I. Kostikov, *Ind. Lab (USSR)*, **39** (1973), 1340.

[65] V. N. Eremenko, *High Temp.* **22** (1984), 705.

[66] P. S. Martsenyuk and Yu. N. Ivashchenko, *Adgez. Rasp. Paika Mater.*, **20** (1988), 15.

[67] S. G. Gushchin, N. A. Vatolin, E. L. Dubinin, and A. I. Timofeev, *Ogneupory* **12** (1977),49.

[68] P. -F. Paradis, T. Ishikawa, and S. Yoda, "Surface tension and viscosity of liquid and undercooled tantalum measured by a containerless method", in press, *Applied Physics A.*

[69] S. Namba and T. Isobe, "Measurement of surface tension of molten metals by electron bombardment heating", *Sci. Papers I. P. C. R.* **57** (1963), 51-54.

[70] J. C. Kelley and A. Calverley, *SERL-Rep.*, **80** (1959), 53.

[71] P. S. Martsenyuk, Yu. N. Ivashchenko and V. N. Eremenko, *Tep. Vys. Temp.* **12** (1974), 1310.

[72] A. D. Agaev, Dissertation, Moscow Steel and Alloys Institute, 1973.

[73] T. Ishikawa, P.-F. Paradis, and S. Yoda, "Noncontact surface tension and viscosity measurements of rhenium in the liquid and undercooled states", *Appl. Phys. Lett.*, **85**(2004), 5866-5868.

[74] T. A. Apollova, E. L. Dubinin, M. M. Mitko, A. I. Tshegodajev, and L. L. Besukladnikova, *Izv. A. N., Met.*, **6** (1982), 55.

[75] P. S. Martsenyuk, *Inst. Tekh. Probl. Mater. Akad. Nauk SSSR*, (1980), 51-57.

[76] A. D. Agaev, V. I. Kostikov, and V. N. Bobkovski, *Izv. Akad. Nauk. SSSR Metall.* 43 (1980).

[77] V. P. Elyutin, M. A. Maurakh, and V. D. Turov, *Izv. Vyssh. Ucheb. Zaved. Chern. Met.* **8** (1965), 110.

[78] O. V. Demidovich, A. A. Zhuchenko, E. L. Dubinin, N. A. Vatolin and A. I. Timofeev, *Izv. Akad. Nauk. SSSR Met.* **1** (1979), 73.

[79] P.-F. Paradis, T. Ishikawa, S. Yoda, "Viscosity of liquid and undercooled tungsten", , submitted, *Appl. Phys. Lett.*

[80] T. Itami, "Condensed Matter – Liquid Transition Metals and Alloys", in *Condensed Matter Disordered Solids,* edited by S. K.

Srivastava and N. H. March (World Scientific, Singapole, 1995), 123-250.

[*81*] T. Ishikawa, P. -F. Paradis, T. Itami, and S. Yoda, "Thermophysical properties of liquid refractory metals: comparison between hard sphere model calculation and electrostatic levitation measurements", *J. of Chemical Physics*, **118** (2003), 7912-7920.

[*82*] S. Ansell, S. Krishnan, J. K. Weber, J. J. Felten, P. C. Nordine, M. A. Beno, D. L. Price, and M. -L. Saboungi, "Structure of liquid aluminum oxide", *Phys. Rev. Lett.*, **78** (1997), 464.

[*83*] G. Jacobs and I. Egry, "EXAFS studies on undercooled liquid $Co_{80}Pd_{20}$ alloy", *Phys. Rev,*. **B 59** (1999), 3961.

[*84*] T. Schenk, D. Holland-Moritz, V. Simonet, R. Bellissent, and D. M. Herlach, "Icosahedral Short-Range Order in Deeply Undercooled Metallic Melts", *Phys. Rev. Lett.*, **89** (2002), 075507.

[*85*] K. F. Kelton, G. W. Lee, A. K. Gangopadhyay, R. W. Hyers, T. J. Rathz, J. R. Rogers, M. B. Robinson, and D. S. Robinson,"First X-Ray Scattering Studies on Electrostatically Levitated Metallic Liquids: Demonstrated Influence of Local Icosahedral Oder on the Nucleation Barrier", *Phys. Rev. Lett.*, **90** (2003), 195504.

JAXA Research and Development Report
(JAXA-RR-04-024E)

Date of Issue : Mar 31, 2005

Edited and Published by :
Japan Aerospace Exploration Agency
7-44-1 Jindaiji-higashimachi, Chofu-shi,
Tokyo 182-8522 Japan

Printed by :
FUJIWARA PRINTING Co., Ltd.
3-6-4 Fujimidai, Kunitachi-shi, Tokyo 186-0003 Japan

Japan Aerospace Exploration Agency